WIDEBAND NONLINEAR DYNAMIC VIBRATION ABSORBER USING COMBINED SOFTENING AND HARDENING STIFFNESS MECHANISM

ALEX MADI CHUNG

A report submitted
in fulfillment of the requirements for the degree of
Bachelor of Mechanical Engineering

UNIVERSITI TEKNIKAL MALAYSIA MELAKA

2019

DECLARATION

I declare that this project report entitled “Wideband Nonlinear Dynamic Vibration Absorber Using Combined Softening and Hardening Stiffness Mechanism” is the result of my own research except as cited in the references.

Signature: .....

Name: ALEX MADI CHUNG

Date: .....

SUPERVISOR DECLARATION

I hereby declare that I have read this project report and in my opinion this report is sufficient in terms of scope and quality for the award of the degree in Bachelor of Mechanical Engineering

Signature: …….....

Supervisor: ASSOCIATE PROFESSOR DR. ROSZAIDI BIN RAMLAN

Date: ……

DEDICATION

I dedicate this work to:

My parents,

Chung Ah Onn and Sylvia ak Abas

My siblings,

Supervisor who always give support and encouragement,

Associate Professor Dr. Roszaidi bin Ramlan

ABSTRACT

The goal of the present work is to assess the performances of a nonlinear dynamic vibration absorber (NDVA) with combined softening and hardening stiffness mechanism in reducing the vibrations of a beam structure which is fixed at its end. In particular, three mechanisms of DVA are considered which are linear stiffness, softening stiffness and hardening stiffness. The purpose is to clarify if the combined of both nonlinear stiffness shows improvements with respect to the linear dynamic vibration absorber (LDVA) and single NDVA device. The nonlinear stiffness mechanism in NDVA is produced by the interaction force between the magnets. The strength of the nonlinearity can be varied by adjusting the separation gap between the magnets. Quasi-static measurement is used to estimate the linear and nonlinear stiffness of the system through force-deflection graph. Then, experimental results from dynamic measurement are presented to characterize the NDVA when the parameters are varied such as the separation gap and input excitation. The DVA is then attached on a beam structure where it is base-excited using a shaker and the reduction bandwidth on the beam response is measured. From this research, it is found that the bandwidth of a NDVA using combined softening and hardening stiffness mechanism is wider than the bandwidth of the LDVA and individual NDVA.

ABSTRAK

Matlamat penyelidikan ini dilakukan adalah untuk menilai prestasi penyerap getaran dinamik bukan linear dengan gabungan mekanisme memperlembut dan memperkeras untuk mengurangkan getaran struktur rasuk yang diapit pada hujungnya. Terdapat tiga mekanisme penyerap getaran dinamik iaitu proses linear, memperlembut dan memperkeras. Tujuannya adalah untuk menjelaskan sama ada gabungan kedua-dua mekanisme bukan linear menunjukkan penambahbaikan daripada mekanisme linear atau satu mekanisme bukan linear. Proses bukan linear dalam penyerap getaran dinamik dihasilkan oleh daya interaksi antara magnet. Kekuatan pengaruh nonlinear boleh diubah dengan mengubahkan jarak pemisahan antara magnet. Pengukuran kuasi statik digunakan untuk menganggarkan kekejuran linear dan bukan linear sistem melalui graf daya-defleksi. Kemudian, data eksperimen dari pengukuran dinamik telah dibentangkan untuk menunjukkan sifat prestasi penyerap getaran bukan linear apabila parameter berubah seperti jurang pemisahan antara magnet dan amplitud getaran. Peranti itu kemudian diletakkan pada struktur rasuk di mana ia telah menerima getaran daripada alat penggonccang dan kadar pengurangan pada tindakbalas rasuk telah diukur. Kajian ini telah mendapati bahawa prestasi penyerap getaran dinamik bukan linear dengan gabungan mekanisme memperlembut dan memperkeras adalah lebih baik daripada linear atau hanya satu mekanisme bukan linear.

ACKNOWLEDGEMENTS

First and foremost, I would like to take this opportunity to express my sincere acknowledgement to my supervisor, Associate Professor Dr. Roszaidi bin Ramlan from the Faculty of Mechanical Engineering (UTeM) for his supervision, support and encouragement towards the completion of this thesis.

Secondly, I would like to express my deepest gratitude to Mr. Johardi bin Abdul Jabar, the technician from Vibro-Accoustics Laboratory and Mr. Harith bin Mustaffer for their assistance and efforts in all the lab and analysis work. Special thanks to UTeM for providing the financial support and facilities to conduct this project.

Special thanks to all my peers, my beloved father and mother for their moral support in completing this degree. Lastly, thank you to everyone who had been the crucial parts of realization of this project.

TABLE OF CONTENTS

LIST OF TABLES

LIST OF FIGURES

LIST OF ABBREVIATIONS

DVA	Dynamic Vibration Absorber
FRF	Frequency Response Function
LDVA	Linear Dynamic Vibration Absorber
NDVA	Nonlinear Dynamic Vibration Absorber
TMD	Tuned Mass Damper

LIST OF SYMBOLS

F	-	Excitation force
k	-	Stiffness constant
c	-	Damping coefficient
ζ	-	Damping ratio
m	-	Mass
ω	-	Operating frequency
ω_n	-	Natural frequency
Ω	-	Frequency ratio
x	-	Displacement
$\dot{x}$	-	First derivatives of x
$\ddot{x}$	-	Second derivatives of x
A	-	Excitation amplitude
b	-	Harmonic term
β	-	Phase angle
μ	-	Mass ratio
α	-	Nonlinearity value
L	-	Length

b	-	Width
d	-	Thickness
ρ	-	Density
E	-	Modulus of rigidity
A	-	Area
I	-	Second moment of area

CHAPTER 1

INTRODUCTION

1.0 Background

Generally, a vibration is a periodic motion, i.e., a motion which repeats itself in all its particulars after a certain interval of time, called the period of the vibration (Den Hartog, 1956). Vibration is undesirable in most cases since it creates noise and damage a machine component. These effects motivate the engineers from different fields to find a method to control vibration levels since the demands of reliability, comfort, accuracy, and noise reduction are increasing. Vibration problems however are still encountered in this modern era mainly in applications like rotating machinery, construction, and transportation. One of the possible reasons is deviation from the usual operating range of the machine for example a sudden increase operating speed. This will increase the vibration amplitude of the machine and transmit the vibration force to the structure where it is placed. When the vibrating frequency of the machine reaches the natural frequency of the structure, resonance occurs. Resonance is the common cause of structural failure. Schilling (2013) reported in a news article that a building collapsed in Bangladesh was because of the vibration generated from sudden restart of huge generators and thousands of sewing machines after brief power outage. Therefore, it is crucial to master the knowledge of vibration in to encounter and control them.

The dynamic vibration absorber was first invented about a century ago by Frahm (1911). The purpose of the invention was to damp a vibration at resonance which arise in bodies subjected to certain period impacts. It is one of the very simple, low cost and efficient solution invented to dissipate excessive vibration energy. Until today, a lot of research have been conducted to improve the performance of dynamic vibration absorber and a new type of vibration absorber is keep increasing.

1.2 Problem Statement

Vibration control measures can be classified into passive vibration control, active vibration control and semi-active vibration control. Passive vibration control is achieved by altering the mass, stiffness or damping to match the natural frequency of the vibrating structure. It does not require extra energy to be added to the system. Active vibration control is the opposite of vibration control as it requires an energy source to drive active devices continuously such as actuators, sensor and some other electronic controller. The sensor will measure the vibration amplitudes produced and an actuator will act to minimize the vibration amplitudes using a well-defined control strategy. Semi-active vibration control can be defined as a passive vibration control measure in which the stiffness and damping of the absorber is altered by the application of a control signal. It requires smaller amount of energy compare with active vibration control to tune the system. The types, applications, advantages and disadvantages of these vibration absorbers will be discussed in the next chapter.

Many researchers are still trying to explore all the possibilities of the passive vibration absorbers. Previous research papers have described different tuning procedures and optimization techniques depending on the type of primary system. However, the major drawback of a linear

vibration absorber is it has a narrow bandwidth operating frequency. A small change in frequency will result in another resonance. Therefore, a nonlinear vibration absorber with combined hardening and softening mechanism is proposed to increase the bandwidth. The mechanism on how hardening and softening mechanism are generated will be extensively in the thesis.

1.3 Objective

The objectives of this project are as follows:

i. To characterize the dynamic vibration absorber.

ii. To design and develop nonlinear vibration absorber.

iii. To investigate the performance of the nonlinear dynamic vibration absorber.

CHAPTER 2

LITERATURE REVIEW

2.1 Dynamic Vibration Absorber

Basically, a dynamic vibration absorber comprises of an additional weight portion, a rigidity element which is usually a spring and a damping element which is a damper. A rigidity element acts as to generate a reaction force to the inertia force applied to the additional weight portion and a damping element acts as to absorb vibration energy. A single dynamic vibration absorber will only provide a reduction or suppression of vibration in one direction only. In other words, two dynamic vibration absorbers placed on a x – and y- axis of a structure will suppress a vibration in both horizontal and vertical direction (Aida et al., 1994). The desire of a dynamics vibration absorber is to provide a reduction of a vibration in a large rotating elements, particularly such elements that exerts periodic unbalance forces on the foundation (Brewer et al., 1975). The absorber is tuned so that its operating frequency is near to a resonant frequency of a system so that when a resonance happens, the vibration is suppressed or reduced to an acceptable level.

2.2 Linear Vibration Absorber

Roberson (1952) states that “In principle, a linear dynamic vibration absorber is an inertia member coupled to a vibrating system by suitable linear coupling members (usually a

spring and viscous damper).” It provides counteract against a vibration of a system by providing a reaction force equal and opposite to the exciting force which causes the vibration. Den Hartog (1956) described a vibration absorber is a device consisting of a linear spring with a stiffness k, a mass and a damper with a damping constant system. The system was attached on a support machine as shown in Figure 2.1. The vibration absorber provides an equal counteract force at resonance when it is properly tuned to match the excitation frequency of the machine. This equation is shown below. The negative sign indicates that the absorber mass is vibrating at a displacement of *x* and providing an equal but in opposite direction of counteract force which reduces the machine’s vibration.

$$F = -kx \quad (2.1)$$

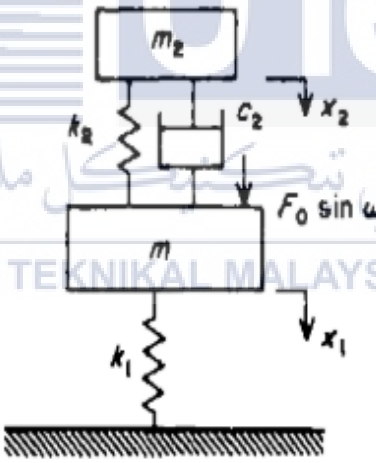

Figure 2.1: Model of a linear dynamic vibration absorber attached to a structure [Source: (Den Hartog, 1956)].

2.2.1 Passive Vibration Absorber

Passive Vibration Absorber is a simple and effective device which is widely used to suppress undesirable machine vibrations excited by harmonic forces. A classic form of passive

vibration absorber has mass-spring-damper configuration. Passive vibration absorber does not require external force or energy. It is activated by the vibrating motion of the structure and acts immediately to dissipate the input energy. Gafsi et al. (2017) presented a design of passive linear vibration absorber to improve the stability of milling tools. The absorber comprises a spring-mass-damper is attached to the milling spindle in x and y axis as shown in Figure 2.2.

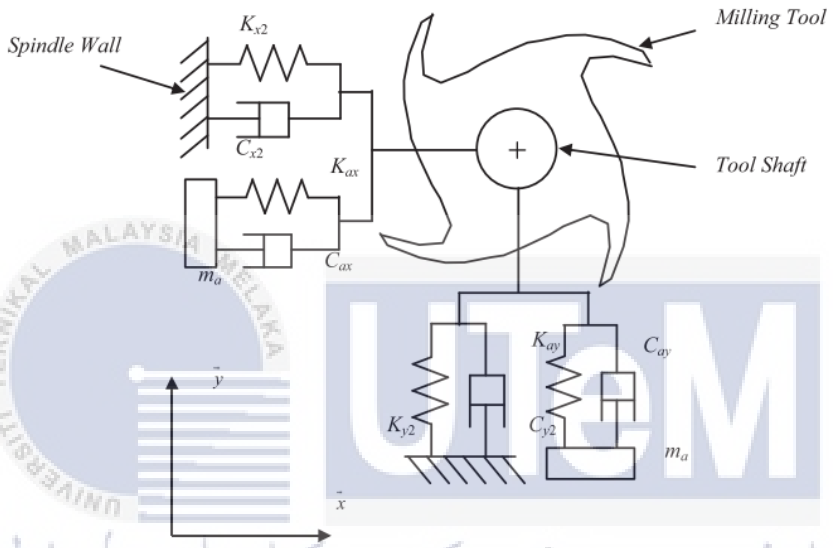

Figure 2.2: Model of the absorber attached on milling tools [Source: (Gafsi et al., 2017)].

The results confirm that the vibration of the milling tool and dynamic loads applied inside the gear transmission is effectively reduced with the vibration absorber. The implementation of the absorber also improves the quality of the work piece surface and reduce the cutting time as the feed rate could be doubled with a slight decrease of tool vibration and the dynamic effort. Fischer (2007) in his journal compare the advantages and disadvantages of different types passive vibration absorber to suppress wind-excited vibration structure. Figure 2.3 shows absorber with translatory mass movement. Any vibration in vertical direction are going to be absorbed by the absorber mass that is suspended vertically on a spring. The mentioned absorber is intended for

bridges. The required damping force is provided by a cylinder immersed in a specific fluid which is well-defined viscosity and little dependent on the temperature.

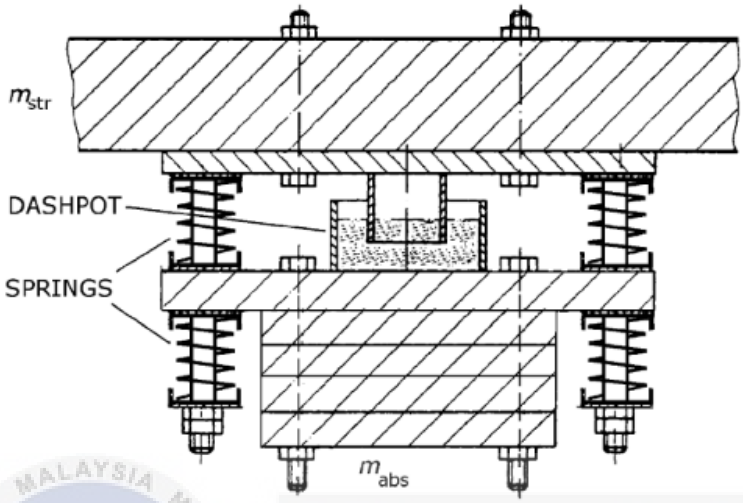

Figure 2.3: Vertical translation vibration absorber [Source: (Fischer, 2007)].

Second type of absorber discussed Fischer is pendulum absorber. Some possible arrangements of the pendulum schematic are shown in Figure 2.4. The damping force required to absorb the vibrations is provided by the motion of a pendulum. However, pendulum absorbers are very difficult to build in tall structures of low natural frequency which they require extremely long or short suspensions.

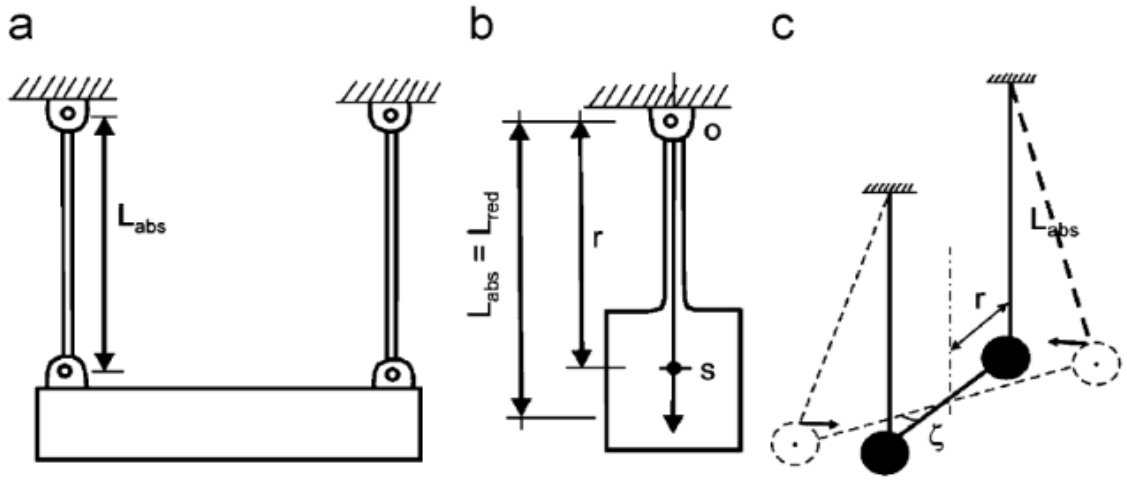

Figure 2.4: Types of pendulum vibration absorbers: (a) translation-mathematical pendulum, (b) swaying- physical pendulum, (c) rotational pendulum [Source: (Fischer, 2007)].

An example of application for pendulum absorber is shown in Figure 2.5 where it is installed to the Taipei 101 to counteract vibration in the building. Poon et al., (2004) explained that it uses building motion to push and pull giant damper and convert motion to heat by forcing the fluid through small internal openings. It is tuned to sway freely at about the same sway rate of the building.

Figure 2.5: Taipei 101 tuned mass damper [Source: (Du Plessis, 2012)].

The ball vibration absorber is an alternative approach to overcome the previous mentioned drawback of pendulum absorber. The pendulum motion is replaced by the motion of sphere in a spherical disc or a cylinder in a cylindrical void. The mass of the rolling body is the mass of the absorber and its frequency depends on the different of ball and dish radii. Pirner (2002) conducted an experiment on a ball absorber as shown in Figure 2.6 on two TV towers. He confirmed it has a good efficiency in counteracting wind-excited vibration and cheap in maintenance cost.

Figure 2.6: The ball absorber designed for a TV tower [Source: (Pirner, 2002)].

However, passive absorber is generally only effective over a narrow frequency band width. As the excitation frequency varies, the performance of the vibration absorber would decrease rapidly due to frequency mistuning. Thus, one traditional method to solve this problem was the development of adaptive or active vibration absorber to widening the effective operational bandwidth (Choy et al., 2017).

2.2.2 Active Vibration Absorber

Generally, an active vibration absorber comprises of sensor and actuator that provide a counteracting force to the primary vibrating structure to reduce its vibration. Compare with passive vibration absorber, active vibration absorber requires external power. A simple block diagram on the principle of active vibration absorber is shown in Figure 2.7. When a sensor detects acceleration from a vibrating structure, the controller will transmit a signal to actuator where it will react to provide a counteract force to reduce its vibration. Active vibration absorber operates by adjusting their own vibrating frequencies to track the changing excitation frequency.

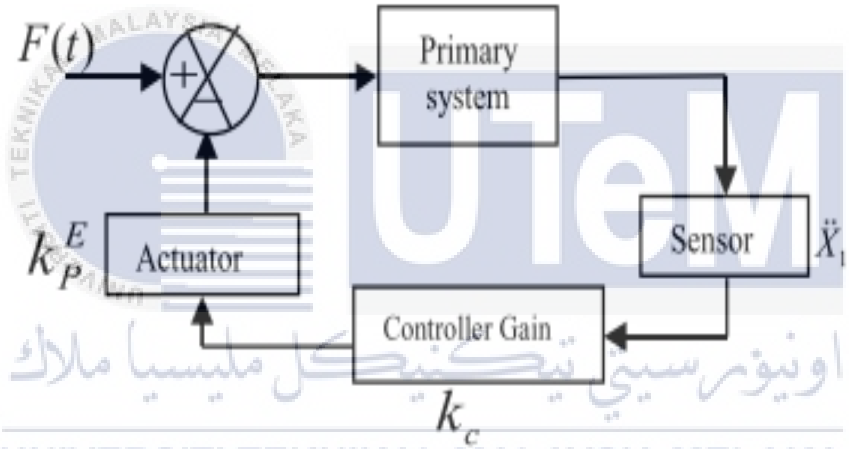

Figure 2.7: Block diagram for acceleration feedback of the primary structure [Source: (Mohanty and Dwivedy, 2016)].

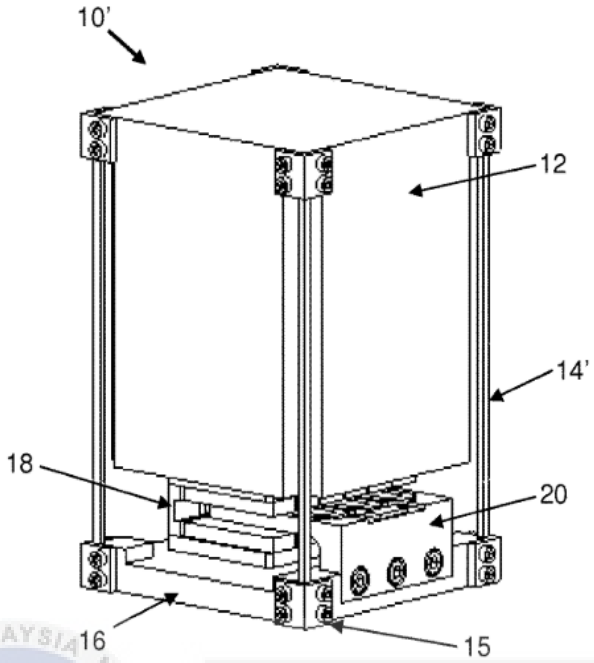

Figure 2.8: Dual axis active vibration absorber [Source: (Choy et al., 2017)].

Choy et al. (2017) have invented a dual-axis active vibration absorber. A schematic view of dual axis active vibration absorber is shown in Figure 2.8. An inertial mass is used to attenuate the vibrations of a structure to which it is attached. An active force component is controlled by an active control system and is positioned between the absorber mass and the primary system of a vibrating structure. The dual-axis active vibration absorber is capable of attenuating vibration in two directions (axes) simultaneously. The advantages of this absorber are it is tunable to a wide range of frequencies which does not require the usage for sensors and complex data processing, much shorter transient time, and small force required to drive the inertial mass.

Mohanty and Dwivedy (2016) proposed an active vibration absorber model consisting Lead Zirconate Titanate (PZT) actuator which is connected in series with spring. The aim was to increase the controlling force developed by the absorber without increasing the piezoelectric stiffness or the voltage parameter. This model was proven to be more economical since one can

use small voltage to reduce the vibration of primary structure and it performs better than the passive dynamic vibration absorber. Gao and Chen (2013) proposed an active controller of cubic velocity time-delayed feedback and a proper design methodology for the controller. Results show that both feedback gain and time delay are important factors for altering dynamics behavior and improving effectiveness of controller.

2.3 Vibration Reduction bandwidth

Roberson (1952) defined the suppression band width as the variation range of operating frequency in which the ratio of $\left[\frac{X_S}{X_0}\right]$ is kept below unity. This region is illustrated in Figure 2.9 by Hsu (2003). It is a frequency response curves of the displacement on the primary system $\left[\frac{X_S}{X_0}\right]$ as a function of a ratio of excitation frequency to the resonance frequency of the system $\Omega = \frac{\omega}{\omega_n}$. The graph also compares the performance between two damping values where the solid line is the low damping absorber whereas the dashed line is the high damping absorber. It can be seen that the low damping absorber is able to suppress vibration greatly which the ratio of $\left[\frac{X_S}{X_0}\right]$ is below unity when the operating frequency is near to the resonance frequency. For high damping absorber, the vibration is not suppressed completely at the same frequency range. However, the low damping absorber will suffer from a higher resonance peaks compare to the high damping absorber. When the operating frequency shifts to frequency near to the natural frequencies of the absorber, another resonance will occur. Therefore, one way to prevent this to increase the resonance bandwidth. One of the effective methods is to use a nonlinear dynamic vibration absorber which is to be discussed in the next topic.

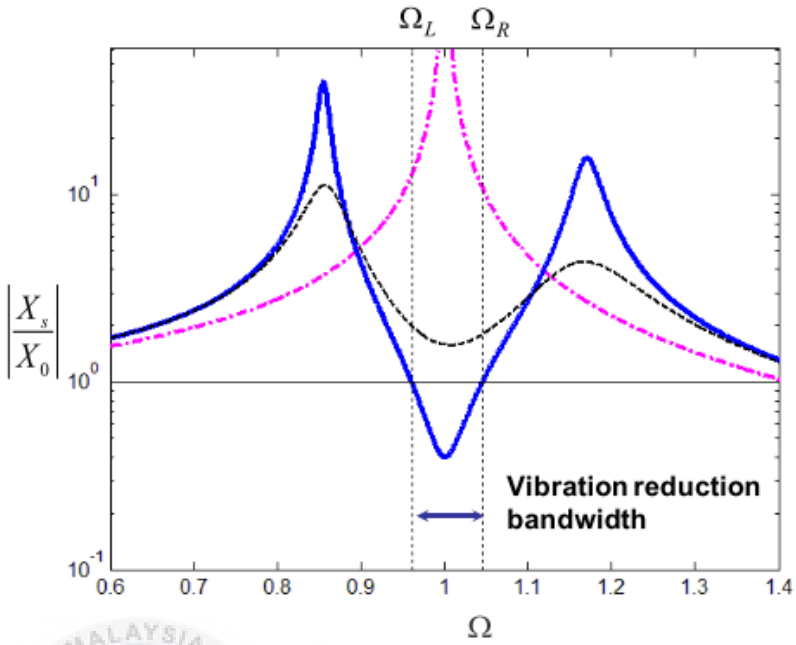

Figure 2.9: Region of the suppression bandwidth [Source: (Hsu, 2003)].

2.4 Nonlinear Vibration Absorber

A linear vibration absorber has a major disadvantage. It is capable to only reduce vibration over a very narrow frequency range which is not convenience to some practical cases that experience changes in the excitation frequency, i.e. in speed for a rotating unbalanced source due to load or motor power supply (Roberson, 1952). Few alternatives have been made to overcome the limitation such as adding the number of vibration absorber. Brewer found that adding more absorbers to the vibrating structure has successfully reduced the vibration level to near zero over wider range of frequency but it has caused another disadvantages which are the increased of overall mass of the system significantly and space limitation (Brewer et al., 1975). Gafsi et al. (2017) suggested to use nonlinear absorbers as well as nonlinear spring in order to improve the performance of vibration absorbers for milling tool vibration.

Tuned vibration absorber is also proven to be effective as a solution to control vibration and broad band application (Sun et al., 1995). Habib et al. (2017) proposed a nonlinear tuned vibration absorber for the suppression of machine tool vibrations. It combines the useful impact of a linear absorber, capable of increase the strong region of operation. Many researchers have conducted a study on a nonlinear vibration absorber to provide a better insight of a nonlinear absorber behavior (Mohanty and Dwivedy, 2016; Tang et al., 2016).

Kojima and Saito (1983) concluded nonlinear vibration absorber has a restoring force of cubic nonlinearity. Roberson (1952) also termed the nonlinear spring as a cubic spring since it produces a restoring force which is proportional to its extension and compression raised to a power of three. Rice and McCraith (1987) presented a nonlinear vibration absorber with third order stiffness for the vibration control of a linear oscillator. Roberson (1952) was among the first to conduct a study of a nonlinear absorber where he considered the effect of both hardening and softening spring in the device. Duffing Iteration Method is used to obtain the first approximation of a nonlinear system which investigates the effect of the parameters of the system. The absorber spring force is

$$k(x \pm \beta^2 x^3) \qquad (2.2)$$

Where *k* is a linear spring constant, β^2 is a constant value and x is the extension of the absorber spring. The result shows that suppression band by nonlinear vibration absorber is seen to be much wider compare to linear vibration absorber. This region is illustrated in Figure 2.10.

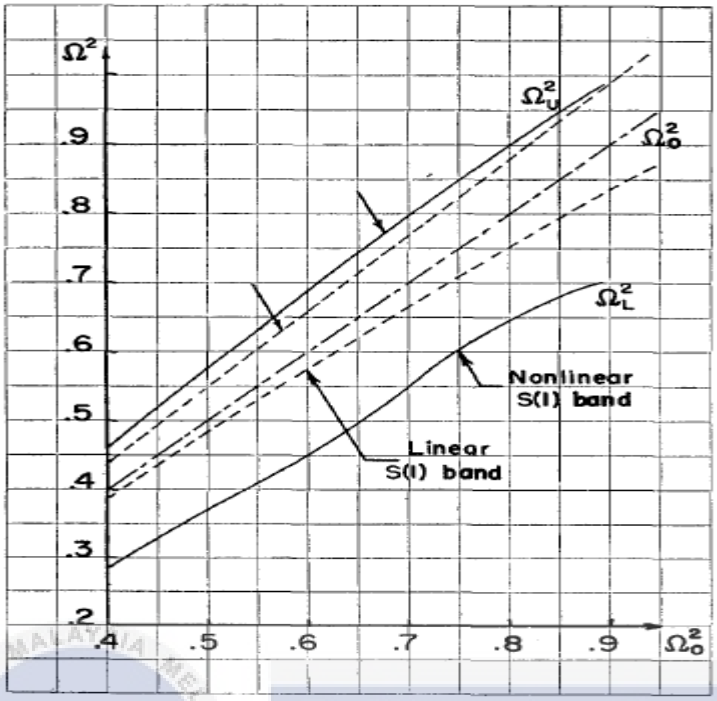

Figure 2.10: Comparison of a suppression bands for the optimum nonlinear absorber and the corresponding linear absorber [Source: (Roberson, 1952)].

Realizing the importance of nonlinear vibration absorber, many studies conducted an experiment using mechanical devices to create the needed nonlinear restoring force, i.e. vibro-impact nonlinear energy sink (NES) (Lee et al., 2009; Gourc et al., 2015), magnetic-strung absorbers (Pennisi et al., 2018), and piezoelectric devices (Soltani and Kerschen, 2015). Soltani and Kerschen (2015) explored the effect of a nonlinear piezoelectric tuned vibration absorber (NPTVA) designed which targets the mitigation of a specific nonlinear resonance of a primary system which is based on the principle of similarity (Habib and Kerschen, 2016). The nonlinear restoring force of the NPTVA is tuned according to the nonlinear restoring force of the primary structure. The NPTVA is found to be able to extend the range of operation toward larger forcing amplitude. Another recent study on a piezoelectric nonlinear energy sink (NES) is proven to be

able to suppress or reduce vibration over a wide range of frequencies as shown by the experimental results and numerical simulation (Silva et al., 2018).

2.4.1 Softening Mechanism

Hunt and Nissen (1982) presented a nonlinear softening spring composed of a Belleville washers in a practical nonlinear vibration absorber to demonstrate suppression bandwidth with comparison to a linear absorber. Nissen et al. (1985) studied the optimal parameters of a NDVA and considered the technical aspects for realization. Hunt and Nissen (1982) and Nissen et al. (1985) provided dynamic vibration absorbers with softening spring (Bellevile washers) to demonstrate wider vibration reduction bandwidth compared to linear absorber. Hunt and Nissen (1982) provided a guidance on the design of the Belleville washer as an absorber spring. Figure 2.11(a) shows a cross-section of Belleville washer. The Belleville washers are stacked back-to-back to form a softening spring as shown in Figure 2.11(b). The Belleville spring is placed in parallel with a viscous damper mounted on a viscously damped primary system as shown in Figure 2.11(c) The response of the system is obtained by a numerical integration solution (Runge-Kutta-Nystrom & Fourier Analysis). As the absorber damping decreases, the result shows that the suppression bandwidth of a nonlinear absorber is doubled as produced by conventional linear absorber as shown in Figure 2.11(d).

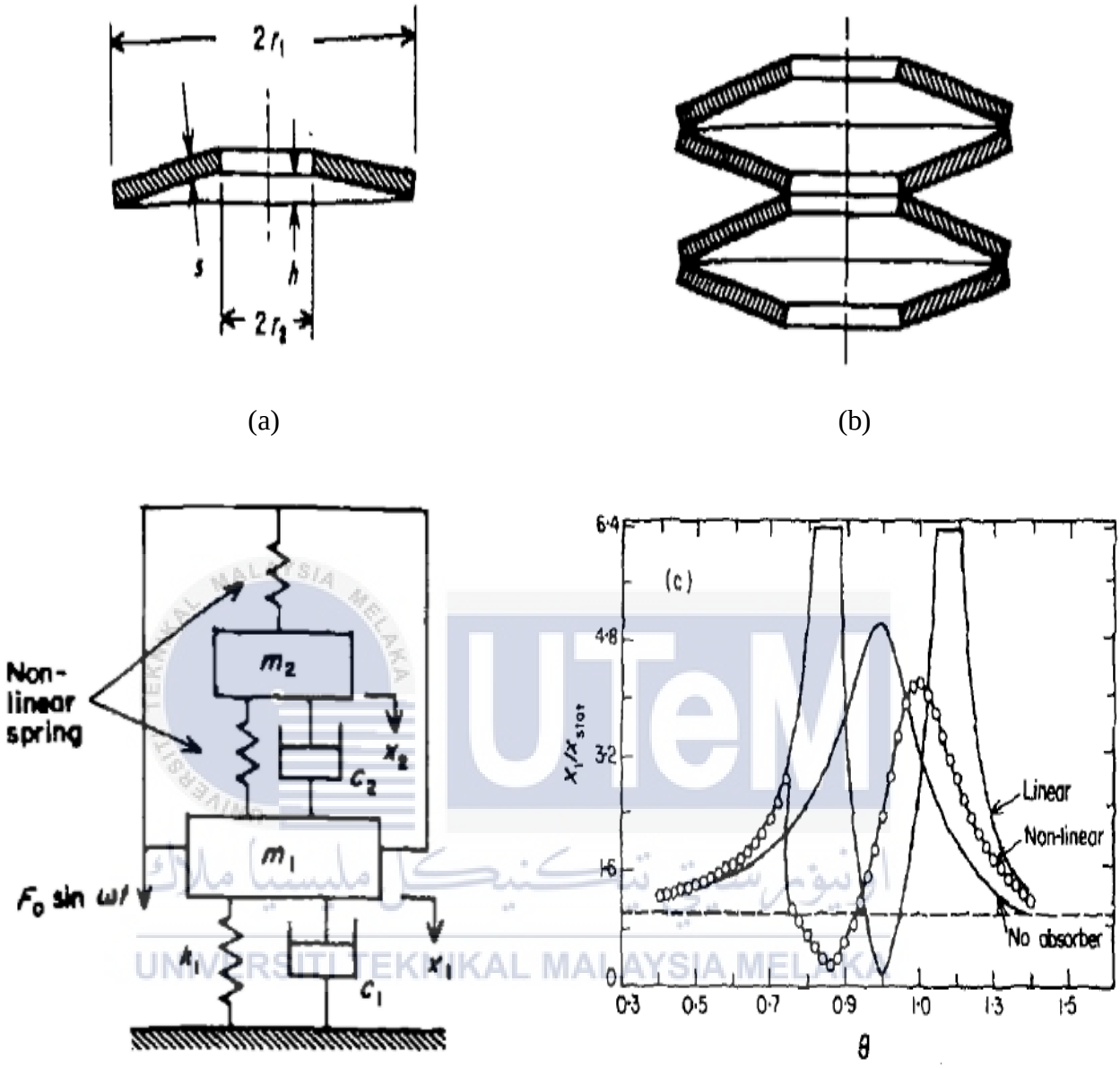

Figure 2.11: (a) Cross-section of a Belleville washer. (b) Stack of Belleville washer. (c) Arrangement of system with attached softening spring. (d) Response curve of a machine fitted with a nonlinear and linear vibration absorber [Source: (Hunt and Nissen, 1982)].

Rice and McCraith (1987) presented the nonlinear vibration absorber incorporating an asymmetric nonlinear element (a linear plus cubic spring) with softening or hardening characteristic and a solution by the harmonic balance method. The spring used is a bow-type or shallow arch spring for narrow-band absorption applications. Their study also found that both hardening and softening absorber are equally good in their capability to increase the suppression bandwidth.

Carter and Liu (1961) analyzed a case for Frahm-type dynamic vibration absorber where both main and absorber springs have nonlinearities of the Duffing type. Figure 2.12 shows a schematic view if the Frahm-type dynamic vibration absorber.

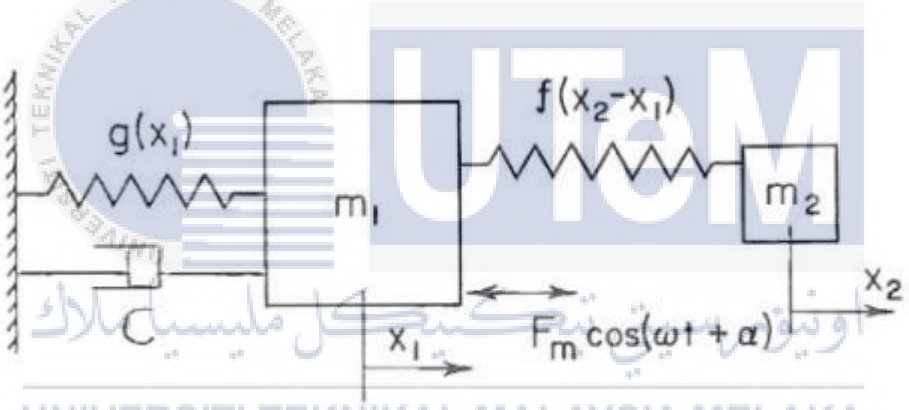

Figure 2.12: Frahm-type dynamic vibration absorber [Source: (Carter and Liu, 1961)].

The differential equations which describe the nonlinearities of the Duffing type are

$$g(x_1) = k_1(x_1 \pm \gamma^2 {x_1}^3) \quad (2.3)$$

$$f(x_2 - x_1) = k_2\,[(x_2 - x_1) \pm \beta^2 (x^2 - x^1)^3] \quad (2.4)$$

where the upper and lower sign is taken for a hardening spring and softening spring respectively whereas γ^2 and β^2 are the coefficient of spring-ratio cubic term of absorber and main spring respectively. From the graphical solution obtained, the combination of softening absorber spring

and hardening main spring is the optimum dynamic vibration absorber for variable frequency since it gives the widest suppression band.

Huang et al. (2018) proved that a dynamic vibration absorber with negatives stiffness is capable to suppress the longitudinal vibration transmission along a marine shafting system under different operating conditions. The proposed DVA model composed of an elastomer pad, a steel mass and Belleville spring as shown in Figure 2.13(a). It is embedded on the dynamic model of longitudinal control for a shafting system as shown in Figure 2.13(b). The Belleville springs provide negative stiffness when they are compressed under the propeller static thrust. Numerical simulations proved that the proposed DVA was capable to suppress vibration transmission for a broader frequency range around resonance with a much smaller size of mass. Inman (2011) found that the restoring force of a nonlinear softening spring is in the form of

$$f(x) = k_1 x - k_3 x^3 \qquad (2.5)$$

Where k_1 and k_3 is a coefficient of linear and nonlinear stiffness respectively.

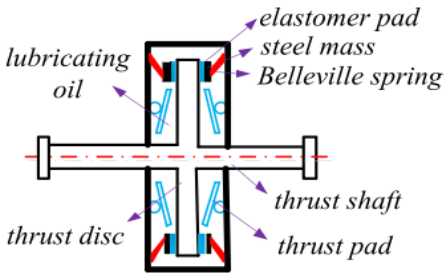

(a)

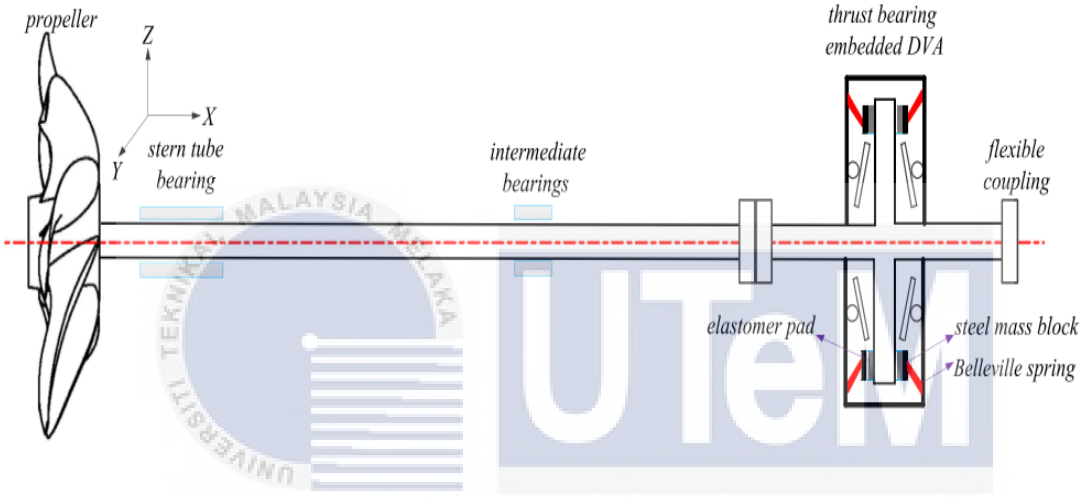

(b)

Figure 2.13: (a) Proposed DVA model with negative stiffness. (b) Dynamic model of longitudinal vibration transmission in a propulsion shafting system [Source: (Huang, Su and Hua, 2018)].

2.4.2 Hardening Mechanism

Many other researchers became interested in nonlinear absorber with hardening characteristic which has a cubic nonlinearity. They believe that it has the same advantages as the softening characteristic has. For example, Alsuwaiyan (2015) presented his work on the effect of hardening spring attached to a vibration absorber in suppressing vibration. The cubic

nonlinearity is achieved by attaching two similar linear spring to the absorber's mass as shown in Figure 2.14(a). Analysis on the dynamic of main structure and the nonlinear absorber was done using the first order harmonic balance method and results were compared against linear absorber. The frequency band width for nonlinear absorber is almost doubled compared to linear absorber as shown in Figure 2.14(b). The results also showed that the displacement amplitude of the nonlinear absorber is decreased when running. Another important finding is as the nonlinearity in the absorber spring stiffness increased, the absorber's effective band width also increased.

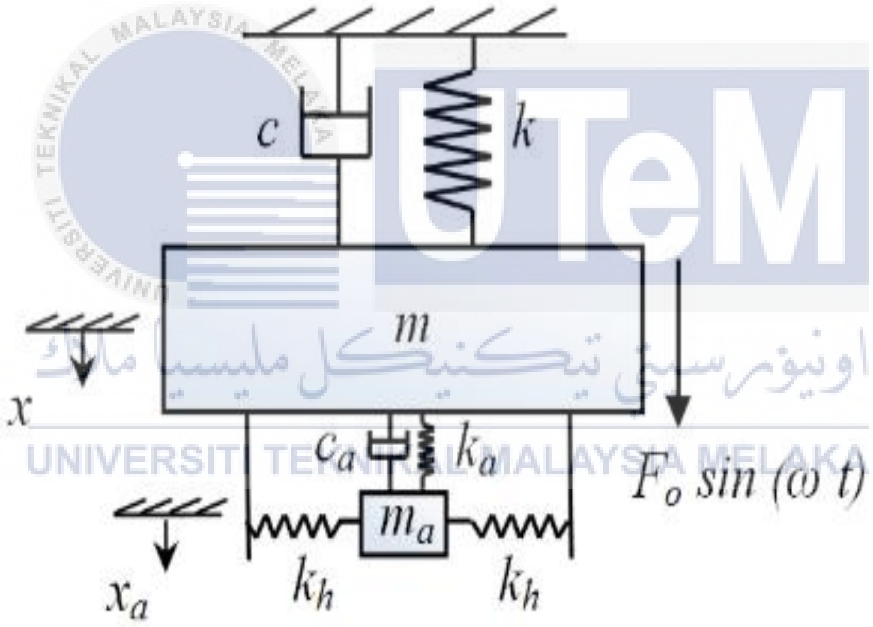

(a)

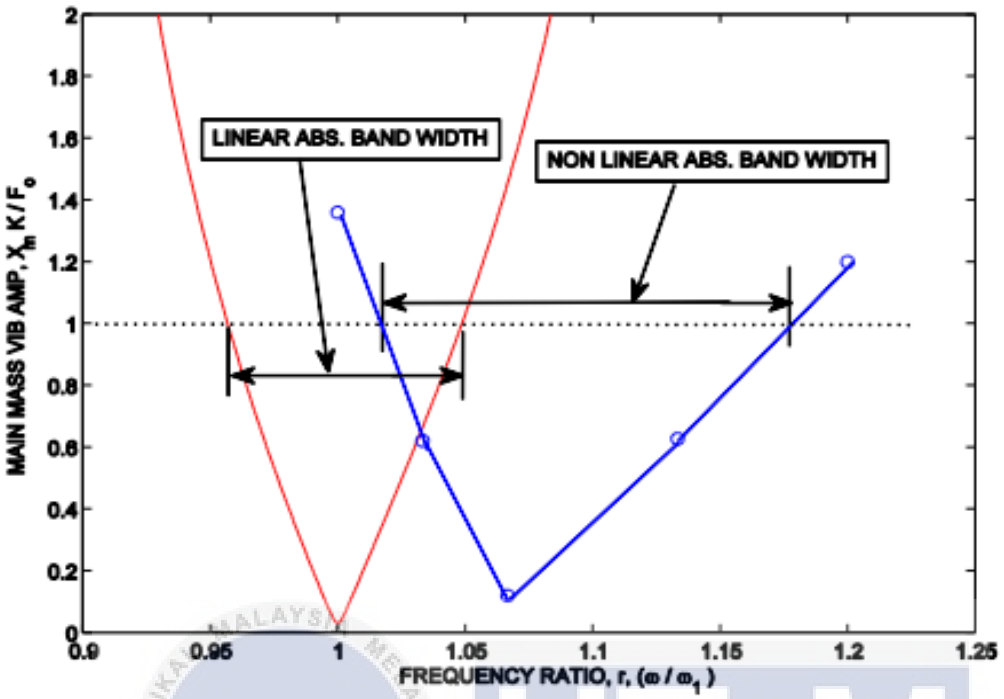

(b)

Figure 2.14:(a) A schematic diagram of the main mass and a nonlinear vibration absorber with hardening effect. (b) Structure amplitude of vibration for different frequency ratios with linear and nonlinear absorbers [Source: (Alsuwaiyan, 2015)]

Kojima and Saito (1983) presented a magnetic nonlinear vibration absorber with a hardening characteristic when the magnets are arranged so as to repel each other as shown in Figure 2.15.

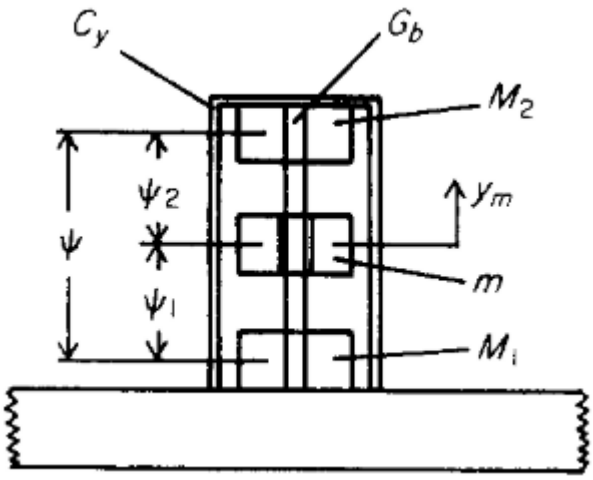

Figure 2.15: Magnetic Nonlinear Vibration Absorber [Source: (Kojima and Saito, 1983)].

It consists of two fixed magnets and one floating magnet. A damping force is generated by the relative motion of the floating magnet and the conductive cylinder. The spring constant, *k* can be varied by manipulating the gap between the two fixed magnets. Jo and Yabuno (2009) also investigated an experimental nonlinear vibration absorber made of repulsive magnets whose natural frequency is twice that of principal system.

Other study that involved the usage of permanent magnets in reducing vibration are investigated by Al-Shideifat (2014). He introduced a new design using asymmetric magnet-based NES and it is proven to be effective in mitigating shock for broadband energy inputs. Two pairs of permanent magnets are aligned to generate a nonlinear magnetic repulsive force. The asymmetric design shows a better performance in energy dissipation for broadband input as compared with the symmetric stiffness-based NES. The stiffness constant of the absorber is a very important parameter in a nonlinear vibration absorber to ensure its effectiveness in minimizing the vibration amplitude at resonance frequency and the absorption frequency range (Roberto et al., 2015). They presented a result where two optimal stiffness (86 N/m and

622 N/m) which are founded through a numerical simulation are used to compare the effectiveness of both nonlinear and linear absorbers. The results show that the second optimal stiffness (622 N/m) shows a wider absorption for frequency as compare to the first optimal stiffness (86 N/m). They conclude that nonlinear absorber is more effective than the linear absorber in terms of reduction the vibration amplitude at resonance frequency and absorption frequency-range. The nonlinear absorber with a hardening spring characteristic shows the right-curved shape on the response curve as shown in Figure 2.16 (Sun et al., 2013).

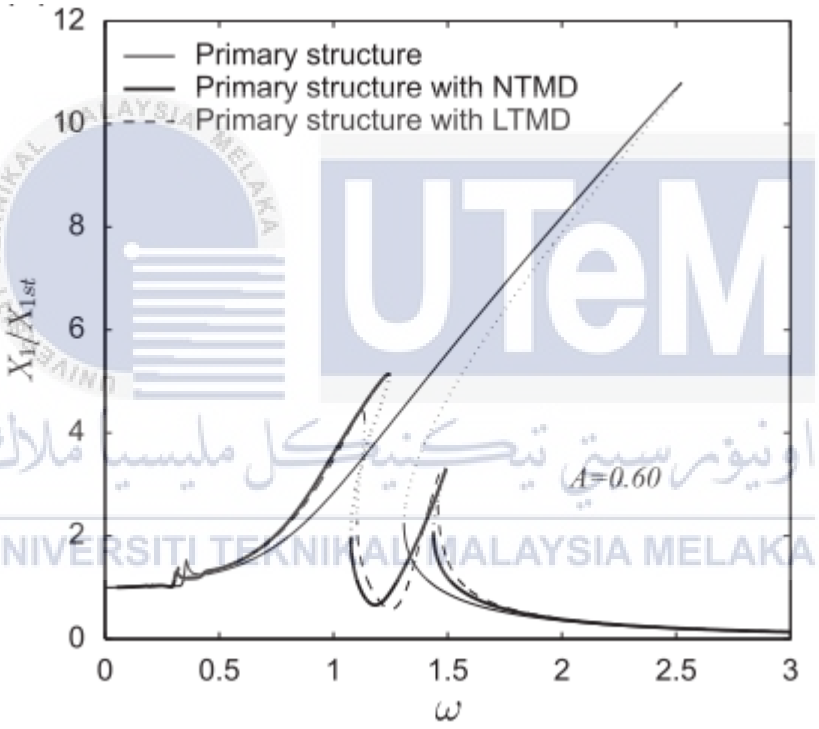

Figure 2.16: Frequency response curve for nonlinear absorber with a hardening spring system [Source: (Sun et al., 2013)].

Yamakawa et al. (1977) presented an absorber consisting of magnets with hardening characteristics using different material of the magnets to investigate the vibration attenuation.

These magnets are arranged in a non-magnetic conductive cylinder in which that one magnet can move freely between the two fixed ones.

Jiang et al. (2003) investigated a nonlinear energy sink (a cubic spring) with hardening characteristics attached to a linear primary structure under sinusoidal excitation both theoretically and experimentally. The result presented that the energy absorption by the nonlinear energy sink, is realized over a relatively broad frequency range making it effective over a range of frequencies compare to the linear vibration absorber whose effect is confined to narrowband.

Jiang et al. (2003) designed a hardening oscillator (a linear plus cubic springs) to investigate the dynamics responses at the resonance frequencies of a nonlinear two degrees-of-freedom system. However, the result could not produce vibration reduction of the primary system as the mass of the nonlinear system was much smaller compared to the mass of the primary system. Hsu (2003) presented a NDVA which is attached to a single degree-of-freedom mass-spring-damper system has a nonlinear restoring force of

$$f(x) = k_1 x + k_3 x^3 \qquad (2.6)$$

where x is the displacement across the spring which has linear and nonlinear stiffness terms k_1 and k_3 respectively. The sign of k_3 denotes the nonlinear stiffness behavior where a positive value means that the system is hardening. Figure 2.17 shows the static restoring force function versus the displacement of the spring for the linear and linear plus nonlinear (cubic) combination.

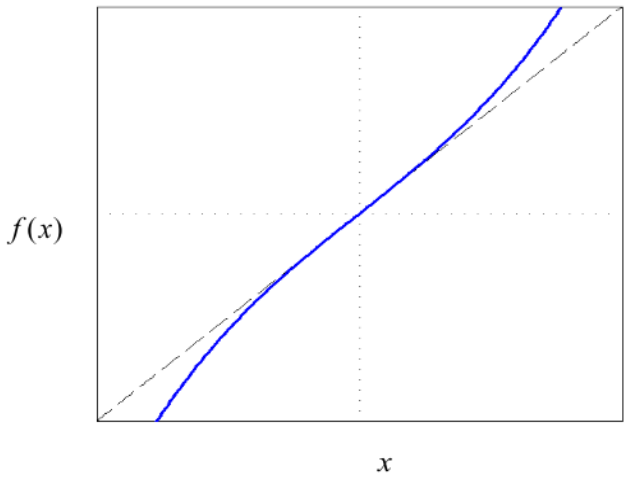

Figure 2.17: Spring force–displacement characteristic of the linear and nonlinear hardening spring types in non-dimensional form. Linear spring: Linear spring: $f(x) = k_1 x$ (dashed line), hardening spring: $f(x) = k_1 x + k_3 x^3$ (solid line) [Source: (Hsu, 2003)].

Ramlan et al. (2016) considered a hardening mechanism which focuses on the determination of the bandwidth using Harmonic Balance Method to solve the equation of motion and obtain the frequency-response relationship. The system consists of mass connected in series with a parallel combination of a damper and a nonlinear spring whose spring force is of the form $k_1 x + k_n x^3$. When $k_n > 0$, the system is denoted as hardening system. The backbone curve bends to the right for the hardening system in a frequency-response curve as shown in Figure 2.18. The analysis showed that the bandwidth of the hardening system depends on the damping ratio, the nonlinearity and the input acceleration.

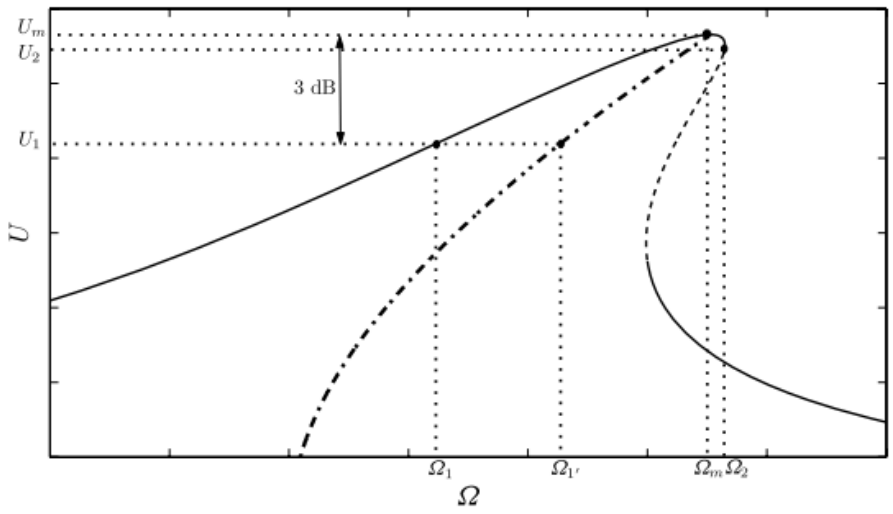

Figure 2.18: Frequency response curve for a hardening system [Source: (Ramlan et al., 2016)].

2.5 Summary

In the literature review, the types of the linear dynamic vibration absorber were introduced. It was divided into passive and active vibration absorber. Their examples, the working principles, the advantages and disadvantages were discussed. Then, a nonlinear dynamic vibration absorber of hardening and softening mechanism were also introduced. The method in producing the hardening and softening mechanism by the previous researchers were highlighted. There has been a wide research effort on nonlinear vibration absorber and the literature cited above is only a fraction of that reported. However, only a few researches on the experimental characterization and finding the benefits of the nonlinear vibration absorber. This is the primary motivation of conducting this research so that a nonlinear vibration absorber will be useful in future. In order for a vibration absorber to be useful, it must have a wide bandwidth and this bandwidth must be wide enough to suppress a range of excitation frequencies during operation.

CHAPTER 3

METHODOLOGY

3.1 Introduction

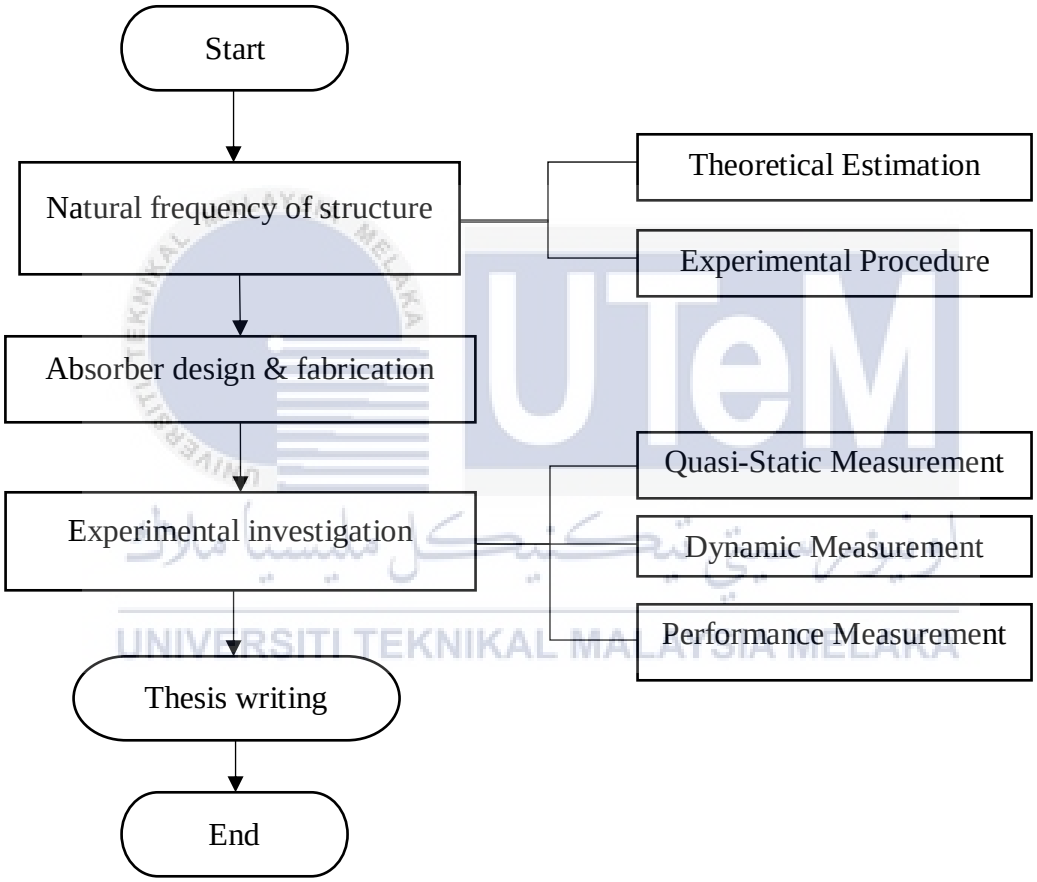

Figure 3.1: Flowchart of the methodology.

This chapter presents the flow of the research methodology in conducting experimentation of the proposed nonlinear dynamic vibration absorber (NDVA). The flowchart of the methodology is shown in Figure 3.1. A beam structure was selected and clamped at its end which represents a cantilever system. Next was to find the natural frequencies of the beam

structure. This was done by theoretical estimation method and experimental method. The mechanism of the DVA was discussed in detail. The experimental investigation was conducted to study the characteristics of the NDVA and to compare their performance. The experiments were quasi-static measurement to find the stiffness of the linear dynamic vibration absorber (LDVA) and NDVA, dynamic measurement to characterize the NDVA when subjected to different parameters and lastly performance measurement to compare the bandwidth reduction between NDVA and LDVA.

3.2 Natural Frequency of the Beam Structure

The natural frequency of the beam structure was determined through theoretical estimation method and experimental method. This was necessary to ensure that the device can be tuned to operate within the first natural frequency of the beam structure. The beam was fixed at specified length as a cantilever system which is illustrated in Figure 3.2. The mechanical properties of the beam structure is listed in Table 3.1.

3.2.1 Theoretical Estimation Method of the Beam Structure Natural Frequency

The first three natural frequencies of the beam structure were estimated by theoretical estimation method. The equations for estimating the natural frequency were obtained from Vlab.amrita.edu (2011).

First natural frequency,

$$\omega_1 = 1.875^2 \sqrt{\frac{EI}{\rho A L^4}} \qquad (3.1)$$

Second natural frequency,

$$\omega_2 = 4.694^2 \sqrt{\frac{EI}{\rho AL^4}} \qquad (3.2)$$

where, E is the modulus of rigidity of the beam material, ρ is the material density, A is the cross section area of the beam, L is the length of beam, I is the second moment of area of a rectangular cross section given as

$$I = \frac{bd^3}{12} \qquad (3.3)$$

where b and d are the breadth and width of the beam cross section.

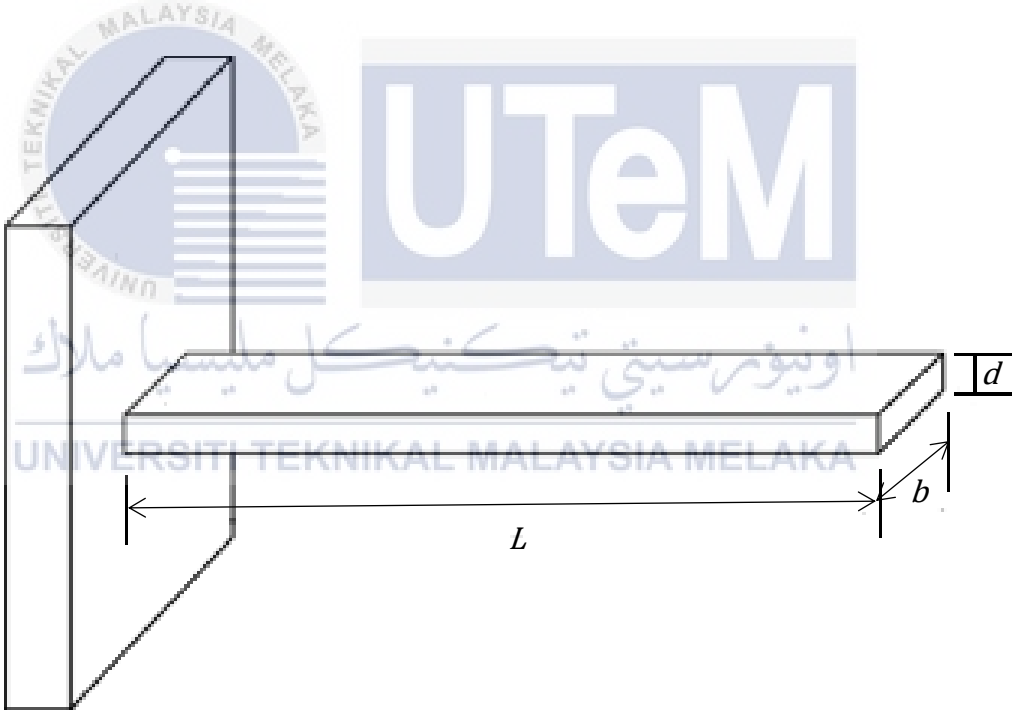

Figure 3.2: Schematic diagram of a cantilever beam.

Table 3.1: Mechanical properties of cantilever beam.

Mechanical properties	Value
Length, L (cm)	70
Thickness, d (cm)	1.2
Width, b (cm)	5.2
Density, ρ (kg/m^3)	7850
Modulus of rigidity, E (GPa)	210

3.2.2 Impact Test

An impact test was carried out to determine the first two natural frequency of the beam structure. An impact test is a quick and easy vibration analysis technique to help identify resonance frequencies in a machine. It requires bumping or hitting the machine or structure when the machine is not in running mode. When impacted, a machine or structure produces a broad frequency band of excitation components. When these frequency components coincide with the structural frequencies, the resonant conditions are present which result in a higher than normal vibration level at those frequencies. The bump test involves using an impact hammer to introduce an excitation force and the accelerometer to measure the result.

A schematic diagram for impact test setup is illustrated in Figure 3.3. The beam was clamped using a G-clamp with the length 70 cm. An impact hammer was connected to Channel 1 of the analyzer and a teflon tip is selected for the test as it provides a greater range frequency of impact. The hammer is instrumented with a force sensor which generates a voltage signal proportional to excitation force so that the excitation is measured during the test. A Dytran accelerometer was attached at the edge of the beam and was connected to Channel 2 of the

analyzer. The impact hammer was then used to hit the beam to induce vibration to the beam. The excitation amplitude of the beam is measured by the accelerometer. The test was conducted with 4 to 6 averages which means the impact hammer was used to hit the beam 4 to 6 times. This was to ensure the measurements taken were consistent throughout the repetition. Averaging also has the advantage of reducing the effect of random noise and does a better estimate of the mean value for each frequency point. Coherence was also monitored during the data acquisition to ensure that the data is valid. The coherence should be close to 1 across the frequency range which indicates that the excitation produces a vibration response that is perfectly correlated to the excitation force. The natural frequencies obtained from the theoretical estimation method and experimental method were compared.

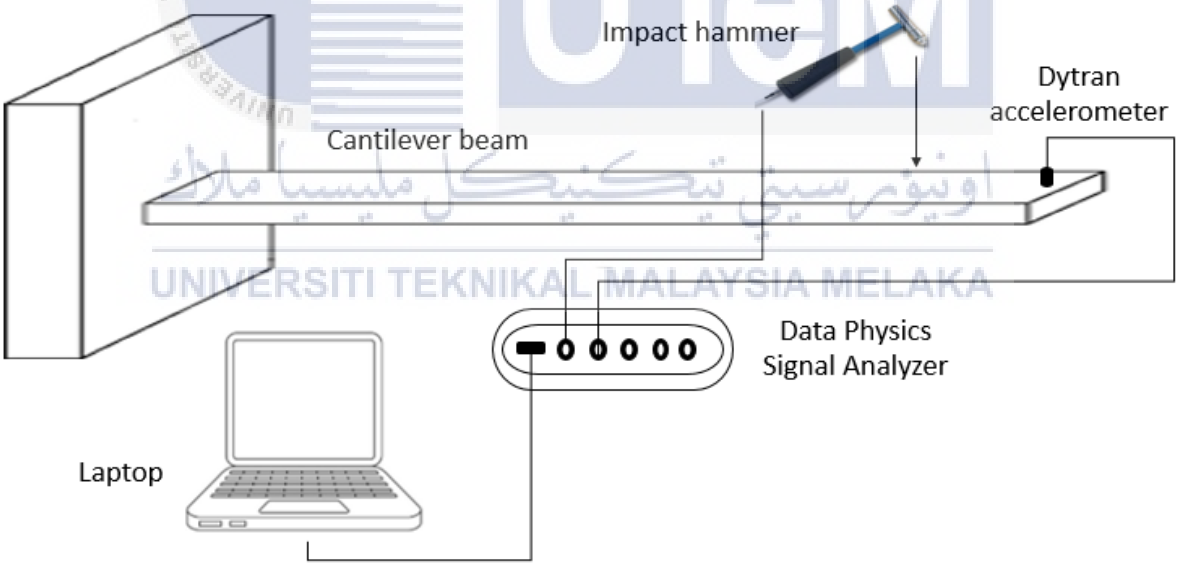

Figure 3.3: Schematic diagram of impact test setup.

3.3 Absorber Design & Fabrication

The actual photo and schematic diagram of a vibration absorber is as shown in Figure 3.4. It comprises of an aluminium cantilever, mass and magnets. The vibration absorber was tuned to the natural frequency of the primary structure by referring to the formula

$$\omega = \sqrt{\frac{k}{m}} \qquad (3.4)$$

The stiffness of the aluminium cantilever was varied until the desired natural frequency was chide. This was done by adjusting the length, L as stated in the formula

$$k = \frac{3EI}{L^3} \qquad (3.5)$$

where E is the modulus of rigidity, I is the second moment of area and L is the length of the aluminium beam. One magnet was attached to the mass at the tip of the beam while another pair of magnet were attached inside the magnet slot at the slider block. The gap, y were varied by adjusting the slider at slider block. The nature of the absorber can be altered to hardening or softening by changing the polarity of the magnets. The absorber will have a restoring force of a softening nature if both of the magnets are the same pole or experiencing a repulsive force, whereas the absorber will have a restoring force of a hardening nature if both of the magnets are the opposite pole or experiencing an attractive force. For confirmation, the absorber is a hardening type if the force increases with the tip deflection or a softening type if the force decreases with the tip deflection. The vibration absorber is a linear type if the attractive or repulsive force between the magnets is removed completely. This was done by adjusting the gap, y until there is no interaction between the magnets or removing one of the magnets. The arrangements for a linear and nonlinear vibration absorber are shown in Figure 3.5.

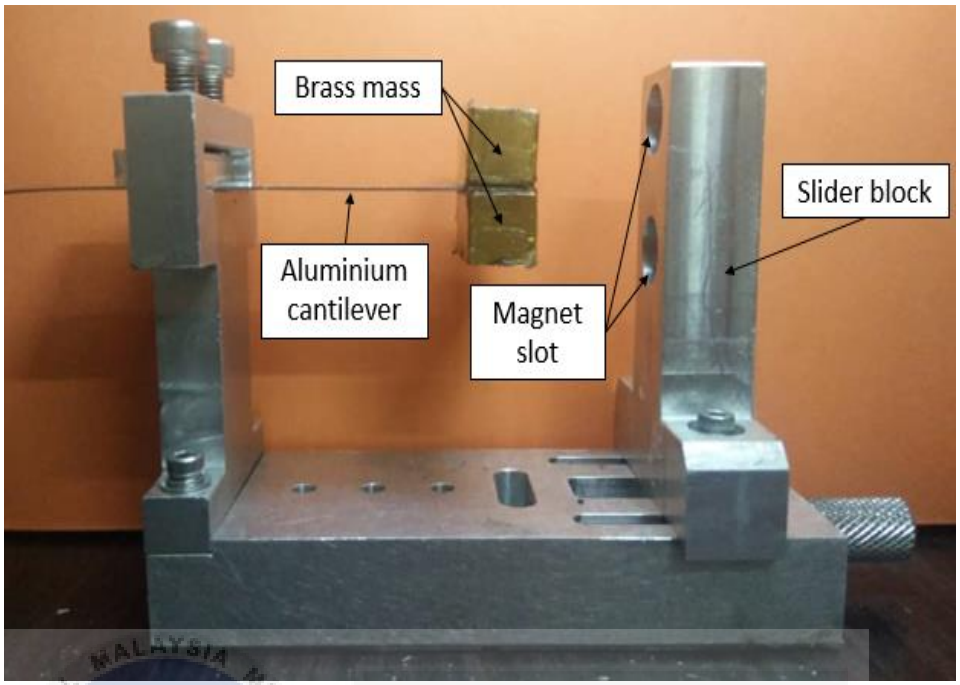

(a)

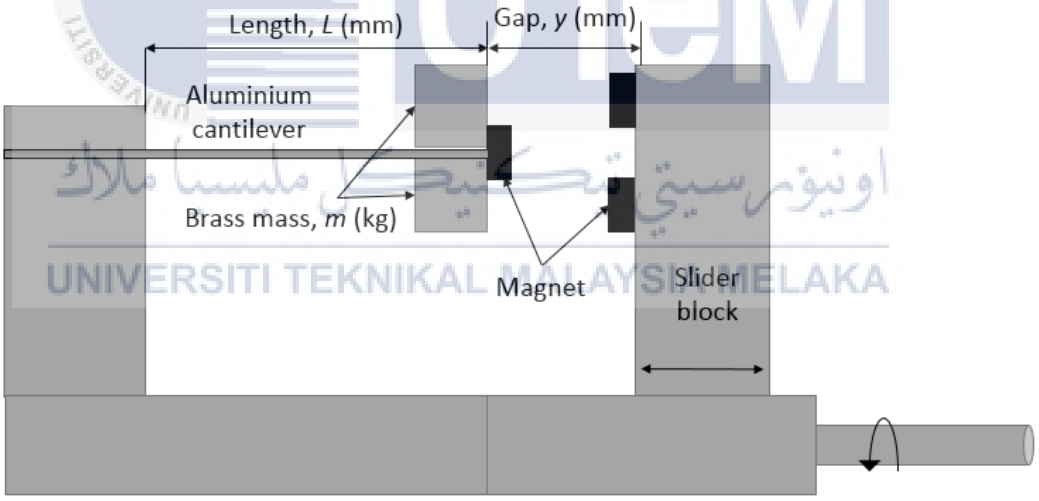

(b)

Figure 3.4: The design of developed vibration absorber model (a) Actual photo of a vibration absorber model, (b) Schematic diagram of vibration absorber model.

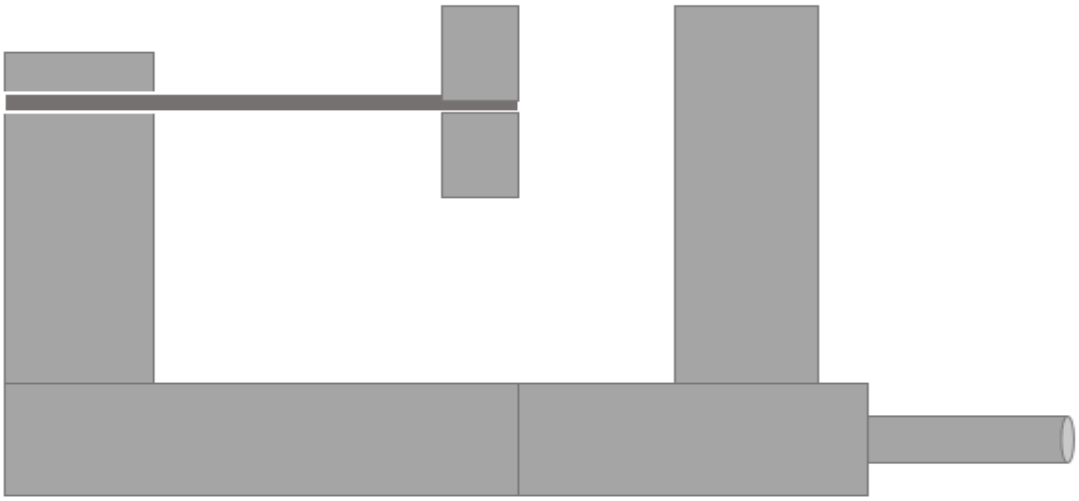

(a)

(b)

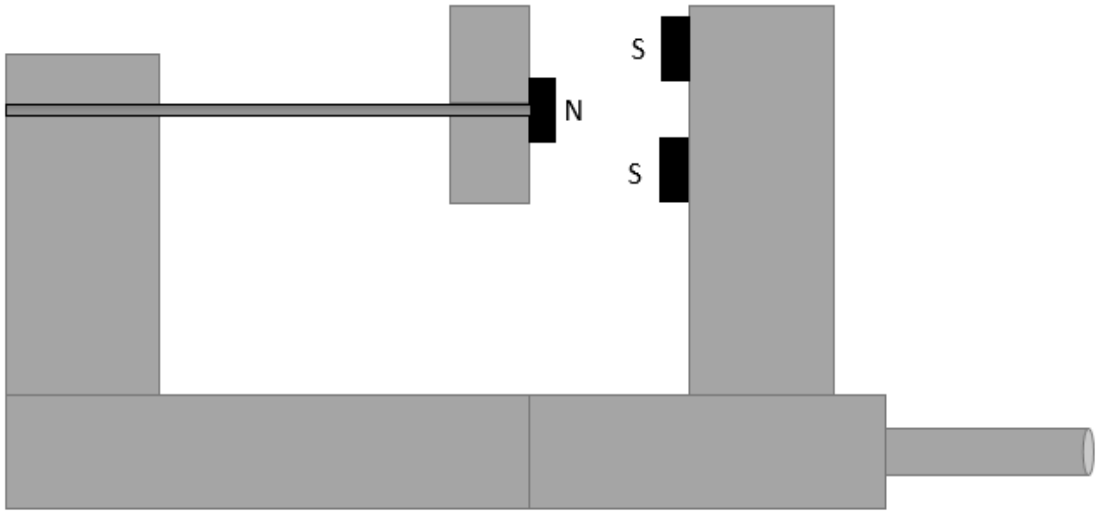

(c)

Figure 3.5: Schematic representation of a (a) linear vibration absorber, (b) nonlinear vibration absorber with softening mechanism, (c) nonlinear vibration absorber with hardening mechanism.

3.3.1 Experimental Method to Obtain Natural Frequency of LDVA

The vibration absorber was tuned to match the first natural frequency of the beam. Figure 3.6 illustrates the set up in finding the natural frequency of the LDVA. The experiment was set up as shown in Figure 3.7. The absorber was attached on top of the base of the ETS electrodynamic shaker where it produces vibration. A Vibration Research Medallion II shaker controller was used to control the vibration output from the shaker and receive signal from the vibration absorber. The first accelerometer was attached on the shaker and connected to Channel 1. It controls the vibration amplitude from the shaker to ensure the input excitation from the shaker to the vibration absorber is constant across the frequency range. The second accelerometer which was connected to Channel 2 is attached on the mass of the vibration absorber to measure its displacement as it vibrates. The shaker was set to excite at low amplitude

which was 0.1 mm with sweep up profile from 10 Hz to 35 Hz. The graph of the displacement amplitude against frequency and phase angle of the absorber mass with respect to the base excitation against frequency were monitored to find the natural frequency of the absorber. The experiment was repeated by adjusting the length of the beam of the vibration absorber until its natural frequency matched the first natural frequency of the beam structure.

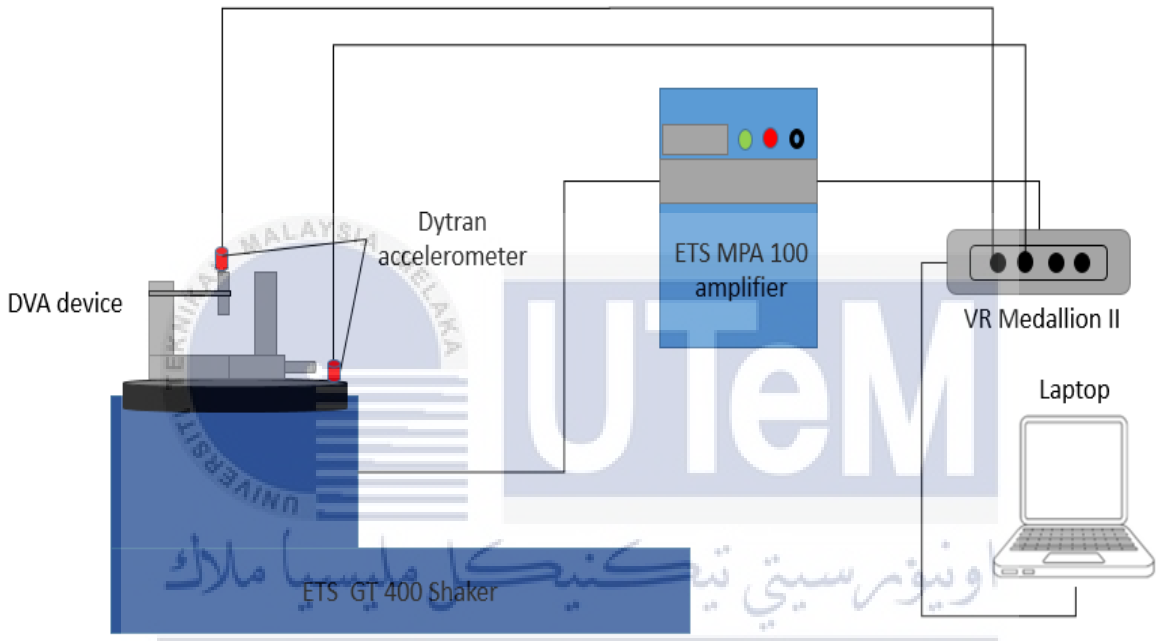

Figure 3.6: Schematic diagram for finding the natural frequency of LDVA.

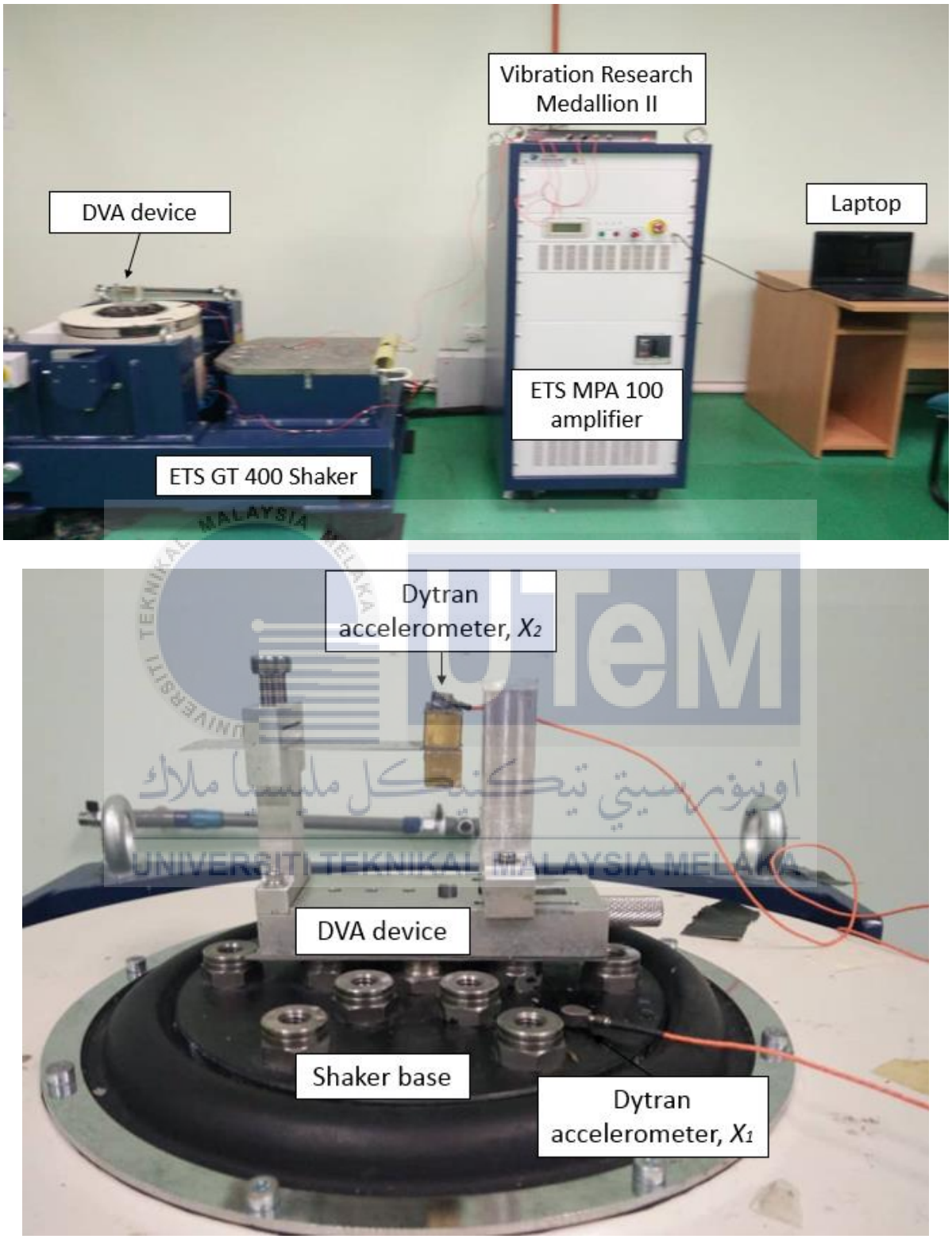

Figure 3.7: Experimental setup for finding the natural frequency of LDVA.

3.4 Experimental Investigation

3.4.1 Quasi-Static Measurement

The quasi-static measurement method was conducted to study the relationship between the restoring force, F against the tip deflection, X_1. This method was adopted from (Ramlan et al., 2016). The base of the DVA was excited at a very low frequency $f < 1$ Hz to ensure the inertial effects are very low and can be ignored.

The quasi-static measurement was set up as shown in Figure 3.8 to estimate the stiffness of the system. The base of the vibration absorber was attached to an electrodynamic shaker (TIRA). The mass at the tip was clamped together with the Tedea-Huntleigh 1042 load cell, to measure the restoring force, F as a result from the deflection. The resulting relative displacement between the tip mass and the base was measured using a Keyence IL-065 laser triangular sensor. The load cell and laser sensor were connected to a 10 V DC power supply. The device was subjected to an amplitude excitation of 8 mm with a frequency of 1 Hz. The output from the load cell and laser sensor were collected by using Data Physics Signal Analyzer. The experiments were conducted according to the parameters setting as listed in the which was different gap, y (mm). The data obtained were plotted in the graph of restoring force, F against the tip deflection, X. The values of the linear stiffness, k_1 and the nonlinear stiffness, k_3 were determined from the slope of the curve.

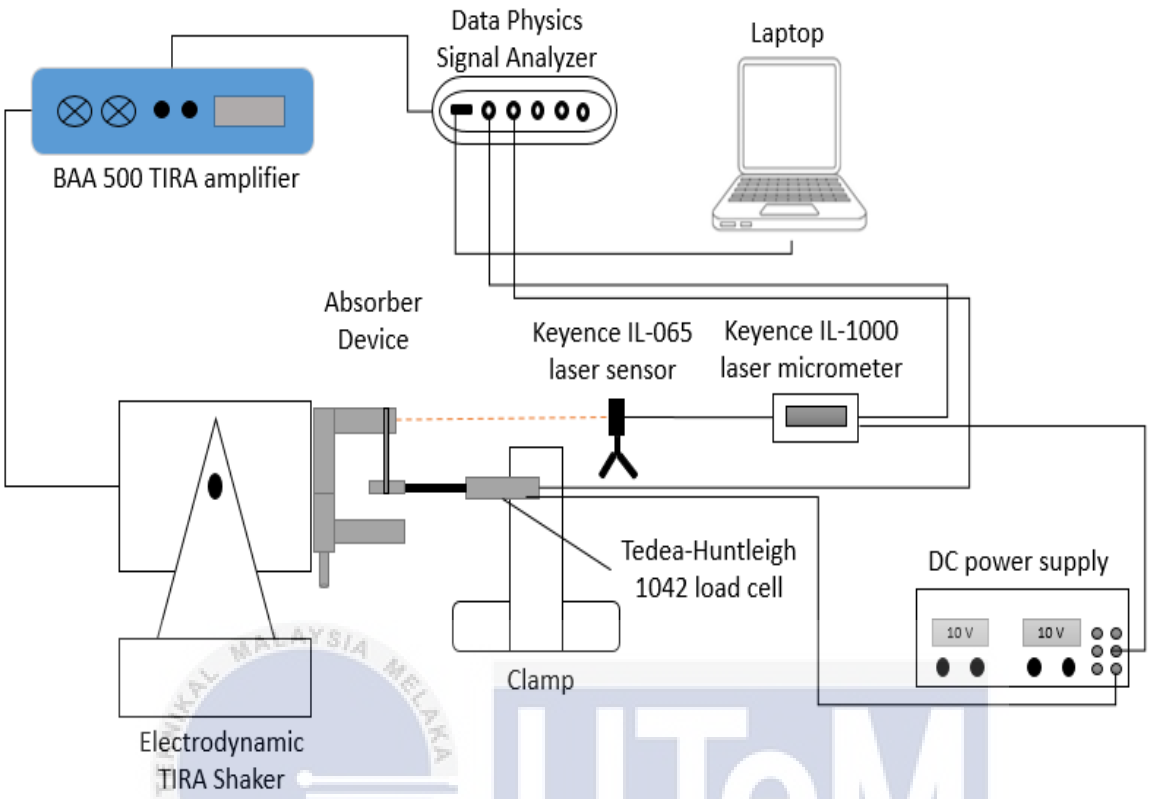

Figure 3.8: Experimental setup for quasi-static measurement

Table 3.2: Variable parameter for static measurement.

Configuration	Gap, y (mm)	k_3 coefficient, (N/mm^3)	k_1 coefficient (N/m)
Linear	N/A		
Attractive	1.0		
	2.0		
	3.0		
	4.0		
Repulsive	1.0		
	2.0		
	3.0		
	4.0		

3.4.2 Dynamic Measurement

In this section, the dynamic measurement was conducted to study the dynamic behavior of the proposed NDVA for each of repulsive and attractive configurations. The experiment characterized the dynamic behavior based on the effect of different input excitation X_1 and different gap between the magnets, y (mm).

The experimental set up is shown in Figure 3.9. The NDVA was firmly attached onto an ETS electrodynamic shaker so that the system was base-excited and the tip mass was free to vibrate. The excitation signal from the shaker was controlled using Vibration Research Medallion II shaker controller which was connected to shaker through ETS MPA100 power amplifier. The NDVA was excited with increasing frequency (sweep up) from 10 Hz to 35 Hz in 0.5 Hz increment and then at decreasing frequency (sweep down) from 35 Hz to 10 Hz with the same frequency decrement. The amplitude of the input displacement was maintained at constant value of 0.5 mm, 1.0 mm and 1.5 mm for all excitation frequencies of interest. A Dytran accelerometer connected to Channel 1 was used to give a feedback on the input excitation, X_1 so that its amplitude can be kept constant all the time. Another Dytran accelerometer connected to Channel 2 was used to measure the acceleration of the tip mass as the test started, X_2. The experiments were conducted based on the variables listed in Table 3.3 which were input excitation and gap. The jump-up frequency, jump-down frequency, and the nature of the NDVA from each variables were recorded in Table 3.3. The data obtained were plotted in the graph of transmissibility, $\frac{X_2}{X_1}$ against f. Schematic diagram for dynamic measurement setup is shown in Figure 3.9.

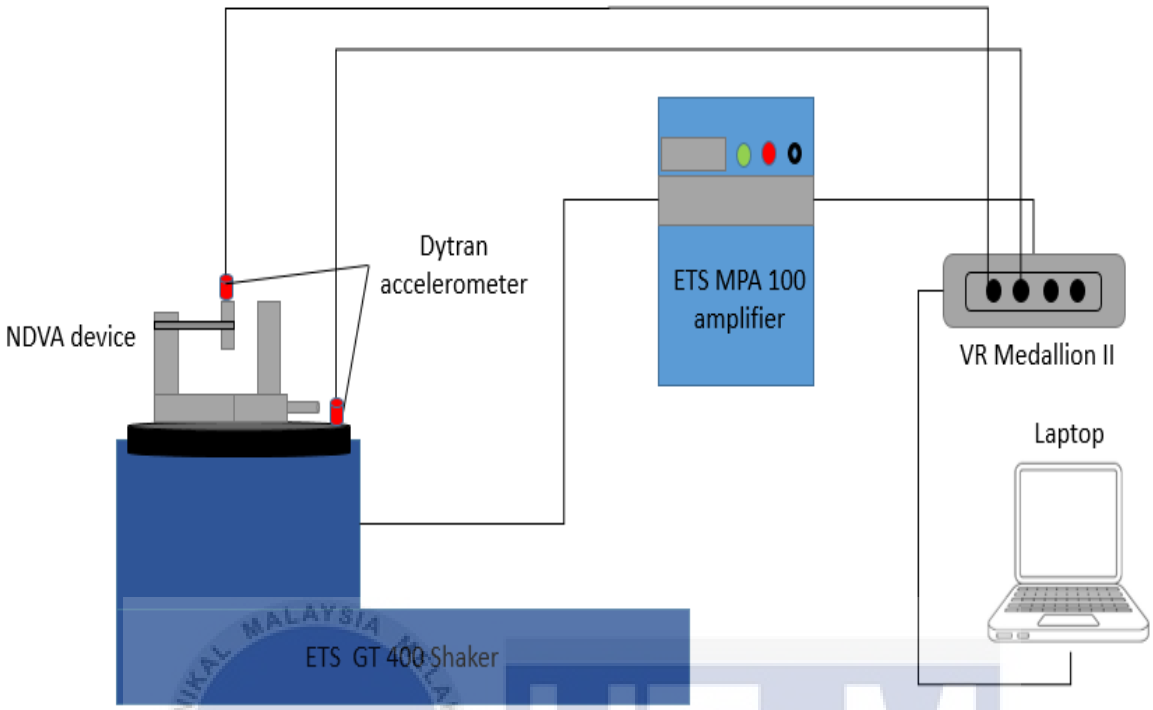

Figure 3.9: Schematic diagram for dynamic measurement.

Table 3.3: List of variables for dynamic measurement.

Configuration	Input Excitation (peak), X_1 (mm)	Gap, y (mm)	Jump-up frequency (Hz)	Jump-down frequency (Hz)	Nature of NDVA
Attractive (N-S)	0.5	1.0			
		2.0			
		3.0			
		4.0			
	1.0	1.0			
		2.0			
		3.0			
		4.0			
	1.5	1.0			
		2.0			
		3.0			
		4.0			
Repulsive (N-N)	0.5	1.0			
		2.0			
		3.0			
		4.0			
	1.0	1.0			
		2.0			
		3.0			
		4.0			
	1.5	1.0			
		2.0			
		3.0			
		4.0			

3.4.3 Performance Measurement of the LDVA and NDVA on the Beam Structure

The experiment was carried out to investigate the performance of the LDVA and NDVA as illustrated in Figure 3.10. This is to prove that the suppression bandwidth of the NDVA using combined softening and hardening stiffness mechanism is wider compare to the LDVA.

The experiment was set up as shown in Figure 3.11. The beam structure was clamped with the same length of 70 cm. TIRA shaker is connected to the beam by using a stinger. Three Dytran accelerometers were attached at the shaker base, beam structure and absorber mass. Dytran force sensor was connected to one end of the stinger and was attached on the beam structure at the driving point. Vibration Research Medallion II shaker controller was used as an analyzer to control the input excitation and to receive signal from the sensors. The device was attached on the beam above the driving point of the shaker as shown in Figure 3.11. The first accelerometer was used to measure the input excitation, X_1 from the shaker and also act as a feedback controller to ensure the amplitude of excitation was constant as the test runs. The input excitation was kept constant at 1 mm for every repetition of the test. The second accelerometer was used to measure the output excitation of the beam structure, X_2 as it received vibration from the shaker. The third accelerometer is attached on the mass of the vibration absorber to see how it the displacement of the mass, X_3 as it vibrates along with the beam. The Dytran force sensor was used to measure the force of the beam structure, F during the excitation period. The test was started first with a LDVA as shown in Figure 3.12(a) where the magnets were completely taken out to remove the effect of the nonlinearity. The LDVA was excited with increasing frequency (sweep up) from 10 Hz to 35 Hz in 0.5 Hz increment. The sweep down test was not carried out for the LDVA as it will produce the same results as in the sweep up test. The NDVA was then tuned to 20 Hz to match the natural frequency of the beam structure. This was done by

changing the length of the beam absorber and until its natural frequency is 20 Hz. The NDVA was excited with increasing frequency (sweep up) from 10 Hz to 35 Hz in 0.5 Hz increment and then at decreasing frequency (sweep down) from 35 Hz to 10 Hz with the same frequency decrement. The NDVA was configured as illustrated in Figure 3.12(b) and Figure 3.12(c). The test was repeated by according to the variable listed in Table 3.4. The final test was repeated using NDVA with combined softening and hardening which were attached on the beam structure as shown if Figure 3.12(d) to investigate performance on the beam structure. The gap that showed the best performance for NDVA of each mechanism was selected for the experiment. The data obtained were plotted in the graph of transmissibility, $\frac{X_2}{F}$ against *f*. The performance of each of the vibration absorber is evaluated at amplitude to force ratio, $\frac{X_2}{F} < 0.10$.

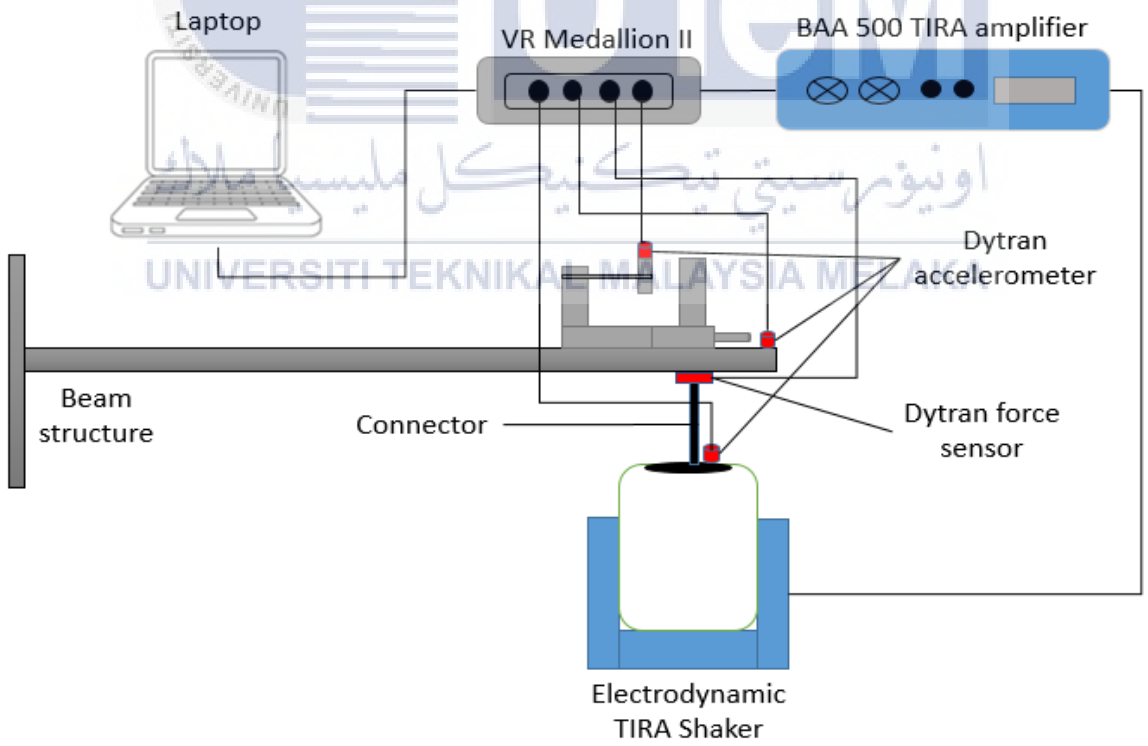

Figure 3.10: Schematic diagram for performance measurement set up.

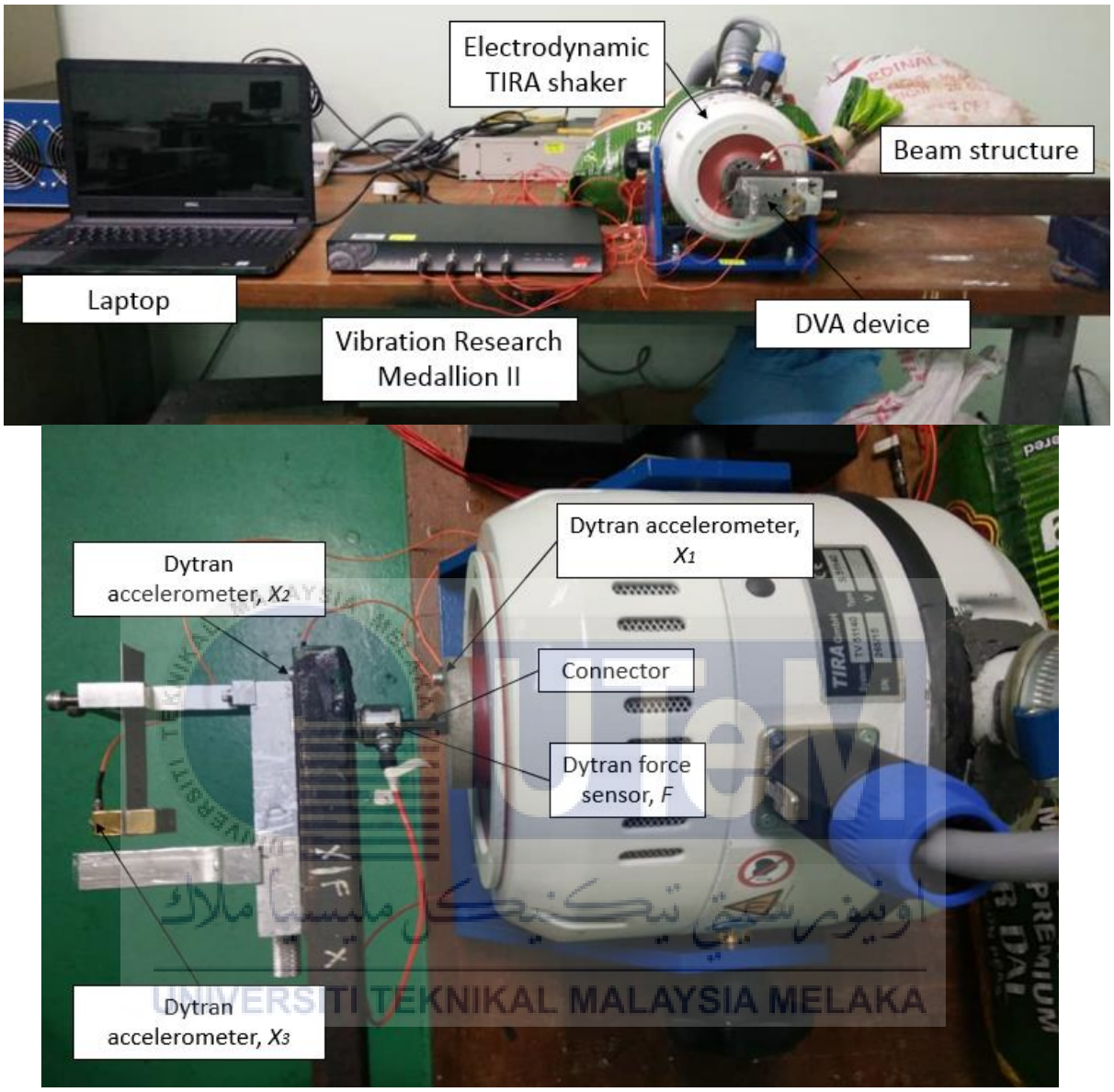

Figure 3.11: Experimental set up for performance measurement.

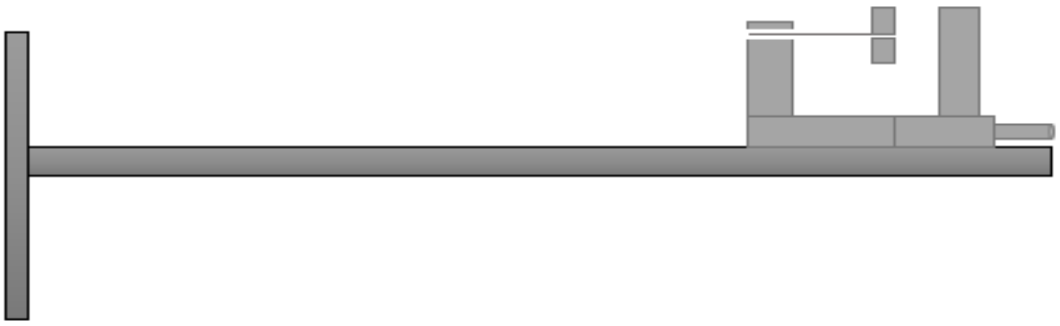

(a)

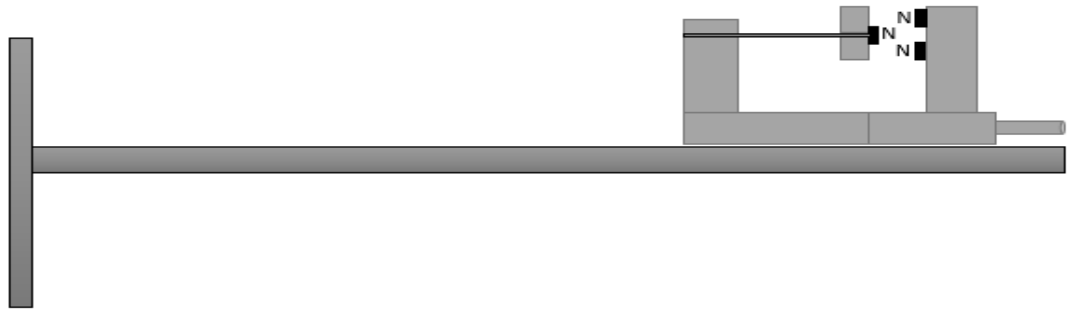

(b)

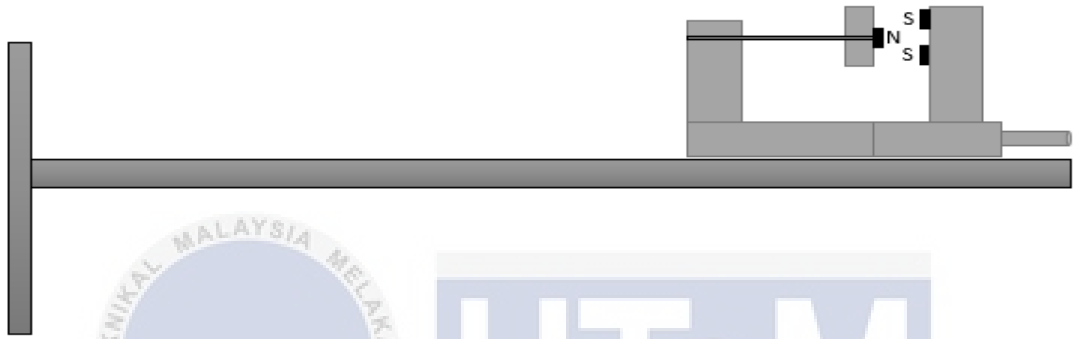

(c)

(d)

Figure 3.12: (a) Experimental on the performance of LDVA. (b) Experimental on the performance of NDVA with softening mechanism. (c) Experimental on the performance of NDVA with hardening mechanism. (d) Experimental on the performance of NDVA with combined softening and hardening stiffness mechanism.

Table 3.4: Variable parameter for performance measurement.

Sweep profile / Gap, *y* (mm)	Vibration reduction bandwidth (Hz)	
	Sweep up	Sweep down
1.0		
2.0		
3.0		
4.0		

3.5 Summary

Throughout this chapter, the methodology of study being conducted has been thoroughly explained. Impact test was carried out to determine the natural frequency of the beam structure. The absorber was tuned by adjusting the length of its beam to match the natural frequency of the beam structure. The quasi-static and dynamic measurement enable us to characterize the NDVA for separation gap and input excitation. The performance measurement was done to measure the effectiveness of the combined NDVA in suppressing vibration. The results obtained is presented and discussed in Chapter 4.

CHAPTER 4

RESULTS AND DISCUSSION

4.1 Introduction

This chapter presents the results and discussion from the experiments that have been carried out. The natural frequency of the beam structure was predicted by theoretical estimation and followed by experiment validation. The natural frequency of the device was then tuned to match the natural frequency of the beam structure through experimental method. Quasi-static measurement was presented in a graph of force-deflection where the value of coefficients of stiffness, k_1 and k_3 were obtained from the equation of the curve. Dynamic measurement was conducted to investigate the behavior of the NDVA when it is subjected to different input excitation and adjusted to a different gap. Finally, reduction bandwidth was compare between LDVA, individual NDVA and combined NDVA mechanism to conclude which system has a better performance.

4.2 Natural Frequency of the Beam Structure

4.2.1 Theoretical Estimation Method

By computing the values from Table 3.1 into Eq. (3.1) and Eq. (3.2), the first natural frequency of the beam structure is 20.5 Hz while the second natural frequency is 128.2 Hz.

4.2.2 Impact test

Figure 4.1(a) shows the frequency response function that measured a ratio of the amplitude excitation with respect to force over frequency range. Figure 4.1(b) shows the phase shifts across the frequency range. It is found that the first resonance of the beam is 20 Hz where it shows the highest amplitude excitation to force ratio and this agrees with Figure 4.1(b) where the is a phase shift of 90 degrees at 20 Hz. A coherence value of 1 at 20 Hz as shown if Figure 4.1(c) confirms that the first natural frequency of the beam is 20 Hz. From the same graph, the second natural frequency of the structure is found to be 129.4 Hz.

It is concluded the first natural frequency of the beam is 20 Hz. The following test will only consider frequencies of interest of 10 Hz to 35 Hz which is enough to cover the first natural frequency of the beam.

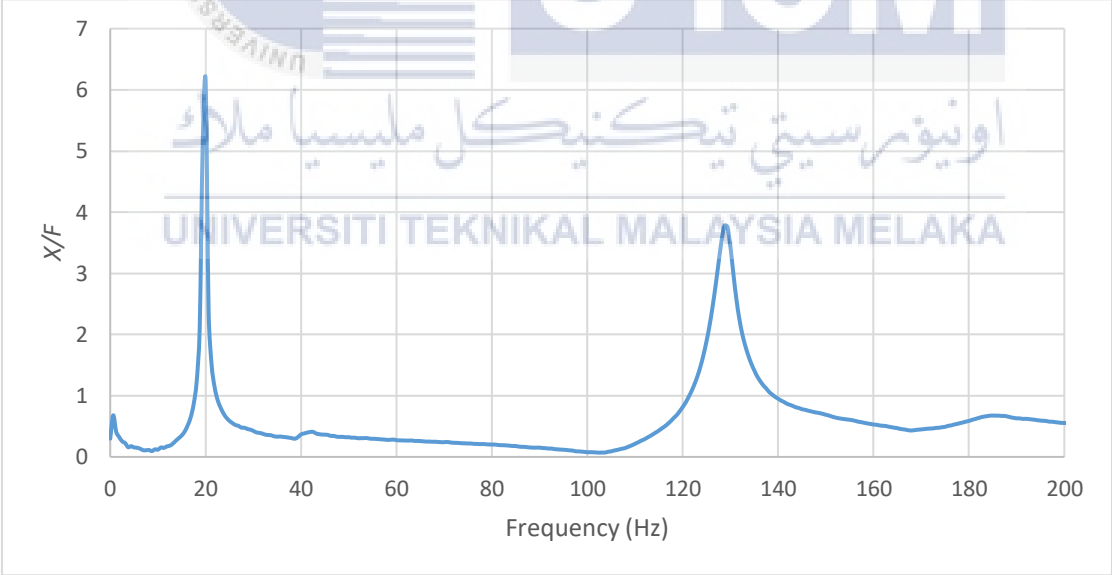

(a)

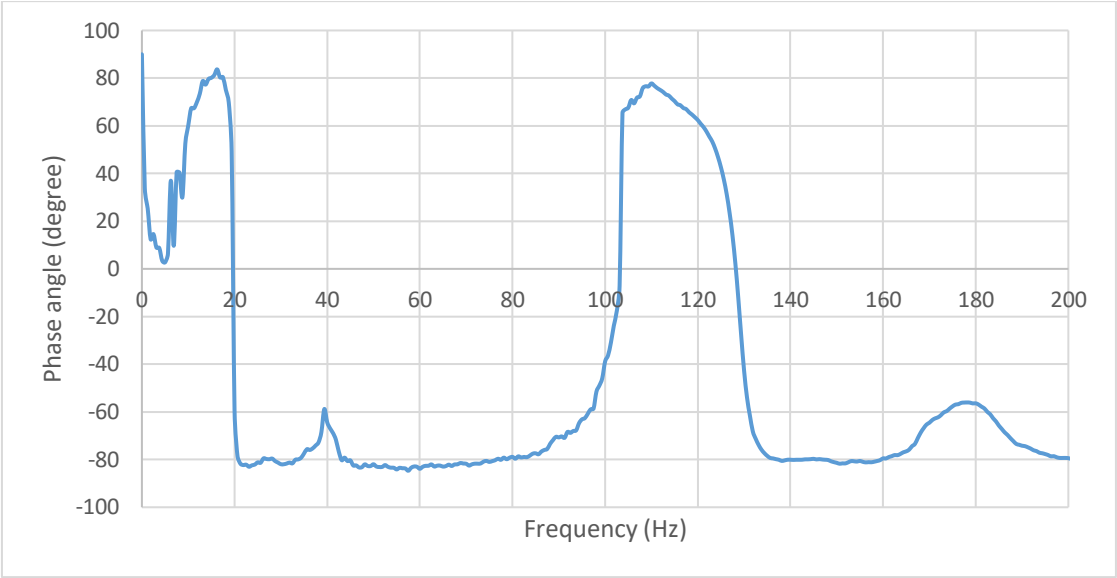

(b)

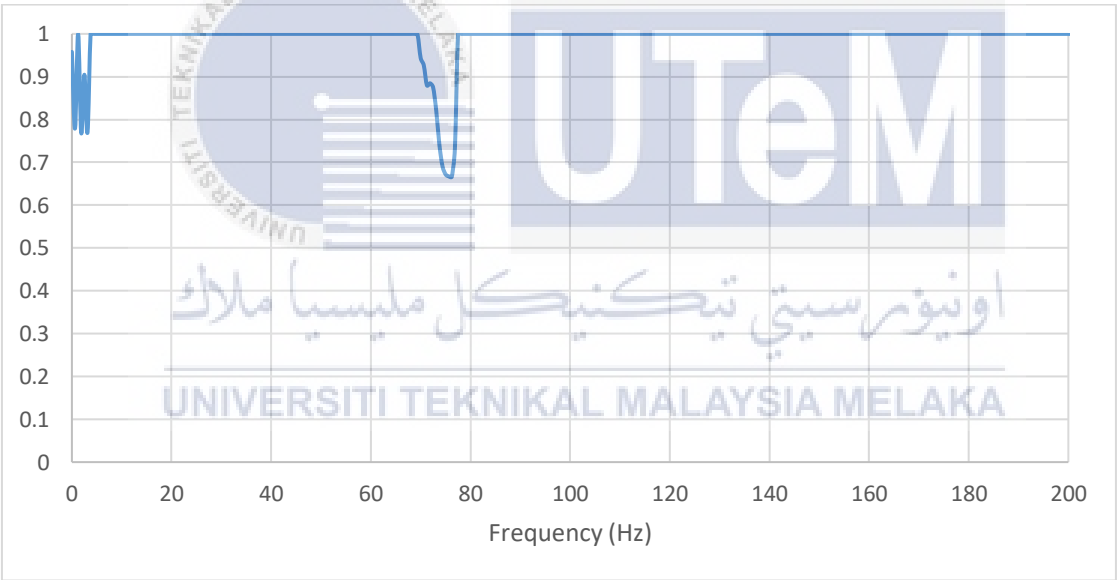

(c)

Figure 4.1: (a) FRF of a beam structure. (b) Phase angle. (c) Coherence

4.3 Natural Frequency of DVA

The LDVA was tuned to match the first natural frequency of the beam structure at 20 Hz. Figure 4.2 shows that at 20 Hz, the displacement amplitude of the absorber mass is the highest which concluded that the experiment was successful.

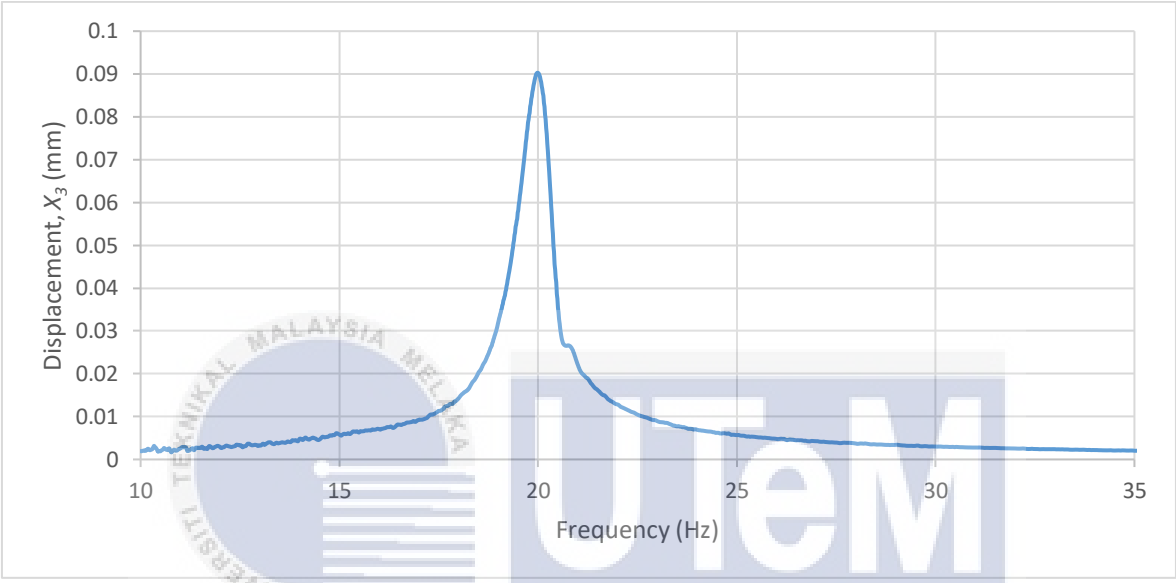

Figure 4.2: Natural frequency of the device.

4.4 Experimental Analysis

4.4.1 Quasi-Static Measurement

This section discussed the results from the quasi-static measurement for LDVA and NDVA. The data obtained were plotted in a restoring force - tip deflection graph. The linear stiffness coefficient, k_1 and nonlinear stiffness coefficient, k_3 were obtained from the slope of the fitted curve. For NDVA, their characteristics were studied as the gap between the magnet was changed.

4.4.1.1 Linear Configuration

The magnets were removed and fitted line of the force-deflection is shown if Figure 4.3. The linear stiffness coefficient for this configuration is found to be k_1 = 1.783 N/mm. By referring to Eqn. (2.1), the equation for the linear system is $F = 1.783x$.

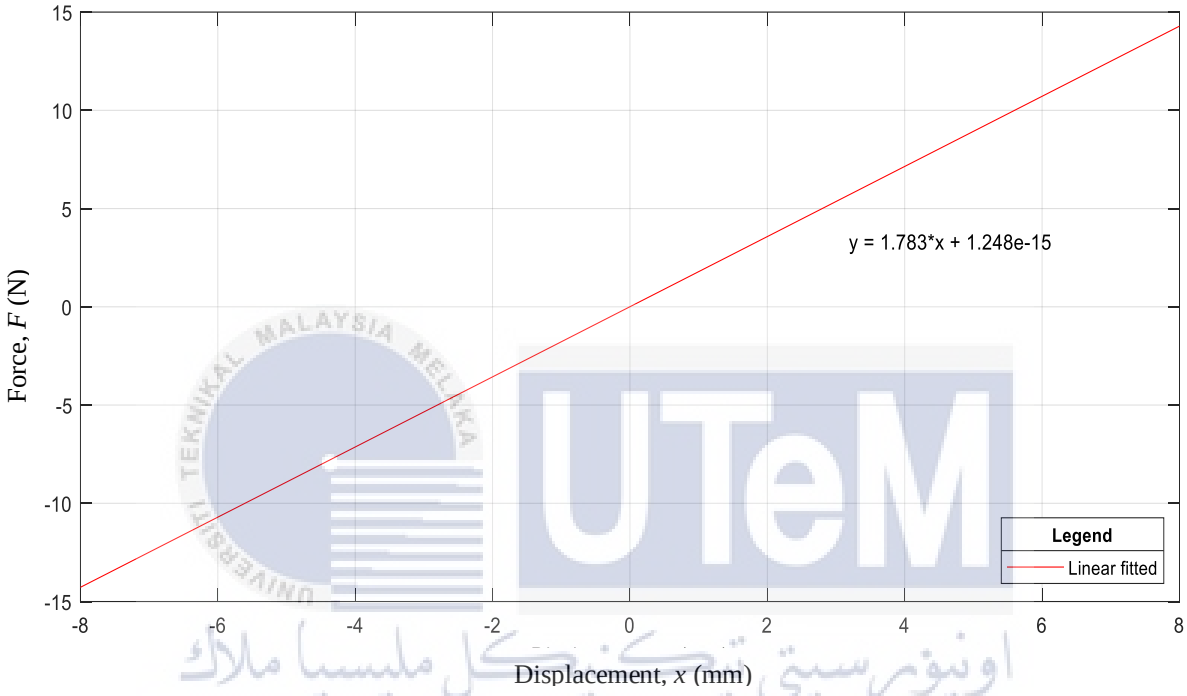

Figure 4.3: Force-deflection curve for LDVA.

4.4.1.2 Repulsive Configuration

Figure 4.4 shows the measured force-deflection plot of the vibration absorber of repulsive magnets arrangement with 1 mm gap between the magnets. The solid curve shows the measured data from the experiment. This curve was then fitted using the least square method with a cubic polynomial using the MATLAB software which is shown by the dashed curve in the figure. The stiffness coefficients for this configuration were found to be k_1 = 4.308 N/mm and k_3 = -0.02044 N/mm^3. The negative coefficient of the k_3 shows that the system with a repulsive configuration gives a softening mechanism effect on the vibration absorber. The steps

were repeated with a 2 mm, 3 mm and 4 mm gap to obtain their respective fitted cubic polynomial curve.

Figure 4.5 shows a fitted cubic polynomial curve for the force – deflection of repulsive configuration. The curve for 1 mm (dotted), 2 mm (dashed dot), 3 mm (solid) and 4 mm (dashed) gap are shown in the graph. The cubic equations and their respective coefficients are listed in Table 4.1. The negative coefficients of k_3 shows that every gap gives a softening mechanism effect as proven by Eqn. (2.5). From the trend, it can be seen that the nonlinearity of the softening is the highest when the gap is 1.0 mm where the magnets are repelling each other with the highest repulsive force. As the separation gap increases for every repetition, the value of the k_3 also decreases. This shows that the absorber is losing its nonlinearity effect as the gap between the magnets become farther. In other words, it is approaching a linear behavior.

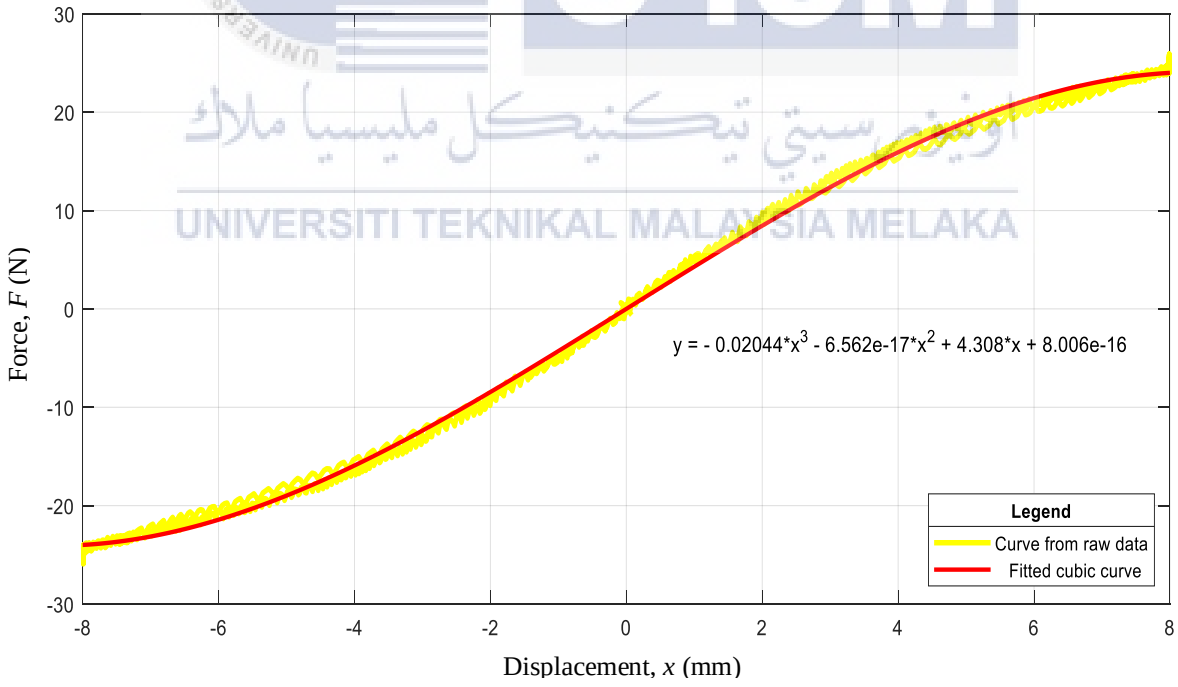

Figure 4.4: Force - deflection curve for the softening stiffness: measured and fitted by cubic polynomial.

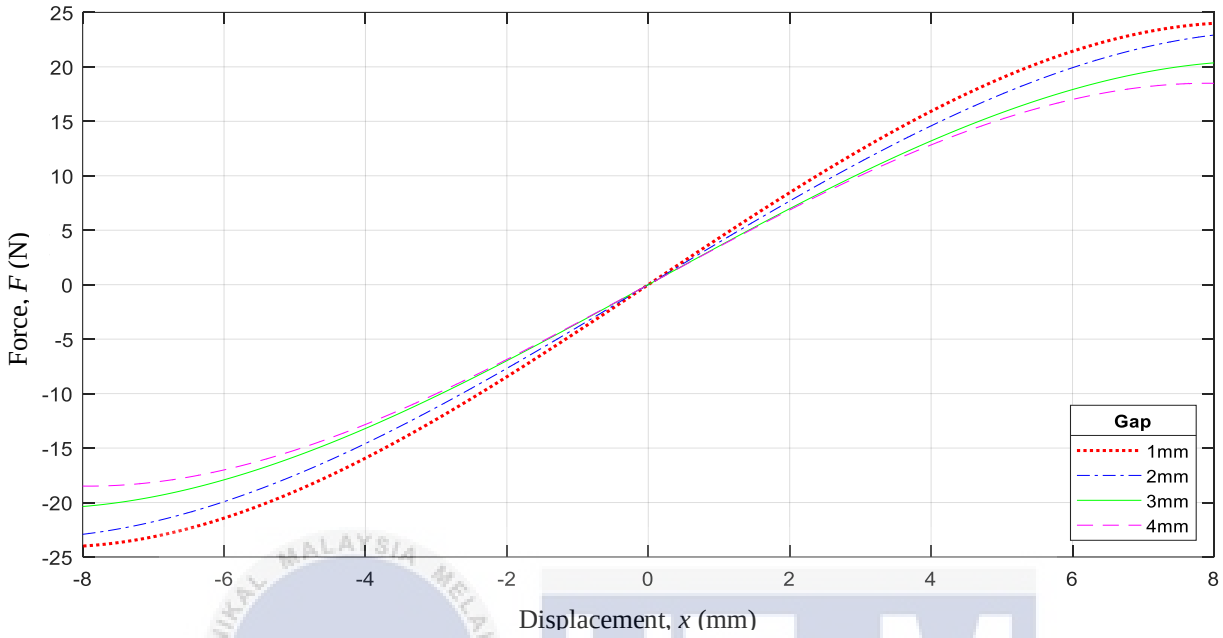

Figure 4.5: Fitted polynomial cubic curve for 1 mm , 2 mm, 3 mm & 4 mm for repulsive magnets arrangement.

Table 4.1: Equations for the fitted polynomial cubic curve for every gap

Gap, y (mm)	Equation from the fitted curve	k_3 coefficient	k_1 coefficient
1	$F = -0.0204x^3 + 4.3076x$	-0.0204	4.308
2	$F = -0.0187x^3 + 3.5066x$	-0.0187	3.507
3	$F = -0.0163x^3 + 3.9058x$	-0.0163	3.906
4	$F = -0.0157x^3 + 3.5514x$	-0.0157	3.551

4.4.1.3 Attractive Configuration

Figure 4.6 shows a fitted cubic polynomial curve for the force – deflection of attractive configuration. The curve for 1 mm (dotted), 2 mm (dashed dot), 3 mm (solid) and 4 mm (dashed) gap are shown in the graph. The cubic equations and their respective coefficients are listed in

Table 4.2. The positive coefficients of k_3 shows that every gap gives a hardening mechanism effect as shown by Eqn. (2.6). From the trend, it can be seen that the nonlinearity of the hardening is the highest when the gap is 1 mm where the magnets are attracting each other with the highest attractive force. As the separation gap increases for every repetition, the value of the k_3 also decrease. This shows that the absorber is losing its nonlinearity effect as the gap between the magnets become farther. In other words, it is also approaching a linear behavior.

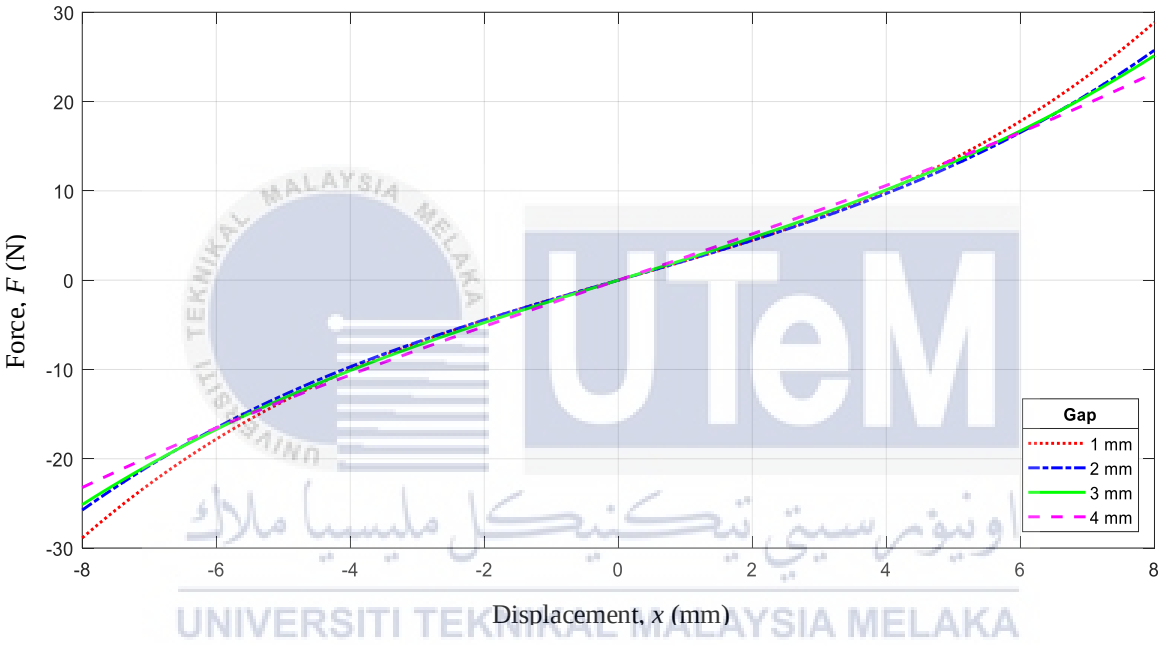

Figure 4.6: Fitted polynomial cubic curve for 1 mm , 2 mm, 3 mm & 4 mm for attractive magnets arrangement.

Table 4.2: Equations for the fitted polynomial cubic curve for every gap.

Gap, y (mm)	Equation from the fitted curve	k_3 coefficient	k_1 coefficient
1	$F = 0.0229x^3 + 2.1411x$	0.0229	2.1411
2	$F = 0.0165x^3 + 2.1633x$	0.0165	2.1633
3	$F = 0.0127x^3 + 2.3269x$	0.0127	2.3269
4	$F = 0.0052x^3 + 2.569x$	0.0052	2.569

4.4.2 Dynamic Measurement

This section presented the results from the dynamic measurement for NDVA. The effect of different input excitation X_1 and different gap between the magnets, y on the dynamic behavior was discussed for each of repulsive and attractive configuration.

4.4.2.1 Effect of Different Gap for Repulsive Configuration

Figure 4.7 shows the graph of $\frac{X_2}{X_1}$ against f under a constant input excitation of 0.5 mm. The response curves bend to the left indicate that the mechanism of the device showed a softening behaviour. In the first test, the device with 1.0 mm gap was excited with a shaker with a sweep up frequency (dashed lines) from 10 Hz to 35 Hz. The first resonance was observed at about 25 Hz with the tip mass was starting to vibrate with large amplitudes. As the frequency was increased beyond this, a second resonance occurred at about 27.1 Hz in which the tip was vibrating at the highest amplidude. This was followed by a sudden drop in motion of the tip mass. This phenomenon is called the jump-down. The frequency was then slowly swept down from 35 Hz to 10 Hz (solid lines) for the second test. A sudden increase in the amplitude of the tip mass was observed at a frequency 17.5 Hz. This phenomena is called the jump-up. These observations were similar obtained by Hsu (2003) and Gatti et al. (2010). The curves bend more to the left during a sweep down frequency compare to sweep up frequency. A similar behaviour were observed for the repetition using the gap of 2.0 mm, 3.0 mm and 4.0 mm but with different jump-up to occur from 14.8 Hz to 17.5 Hz whereas the jump-down to occur from 19.5 Hz to 24.1 Hz. The jump-up and jump-down frequencies were recorded in Table 4.3. The jump-down frequencies shifted to the left whereas the jump-up frequencies shifted to the right for every increment of 1.0 mm gap between the magnets.

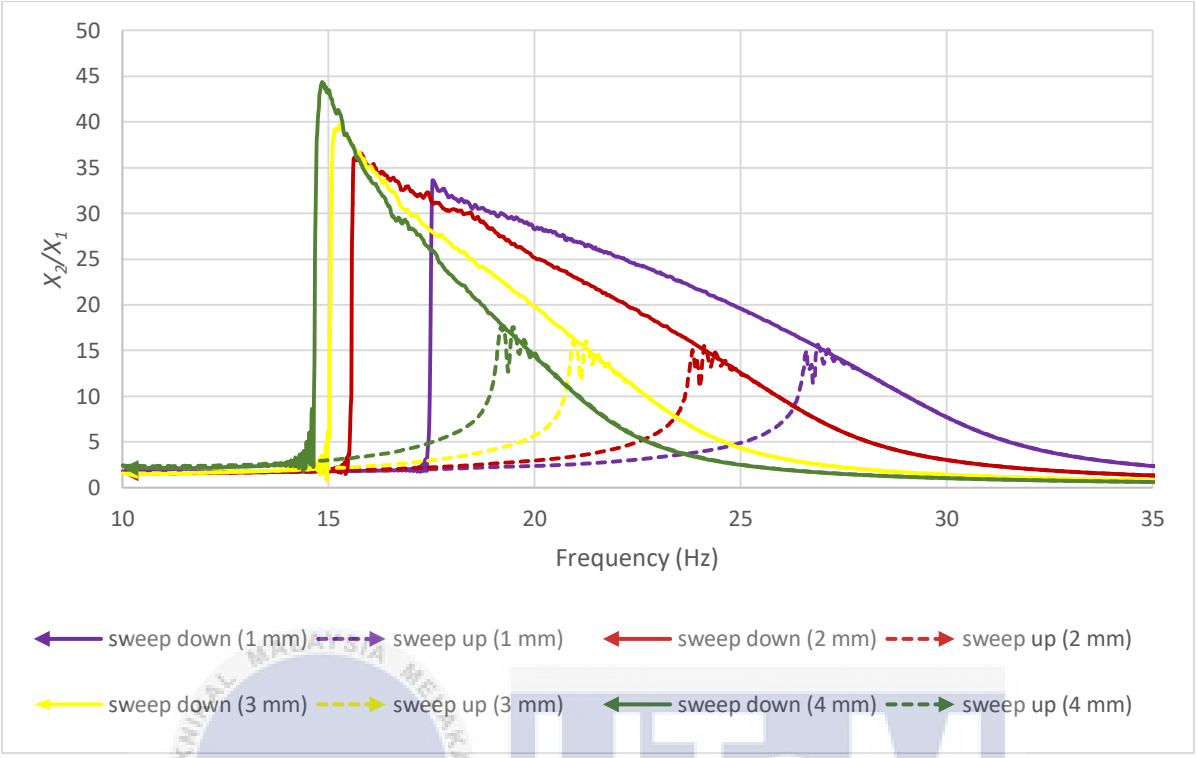

Figure 4.7: Graph of of $\frac{X_2}{X_1}$ *against* f under a constant input excitation of 0.5 mm (peak).

Figure 4.8 shows the graph of $\frac{X_2}{X_1}$ against f under a constant input excitation of 1.0 mm. The jump-up freqeuncies occurred in the range of 15.7 Hz to 18.7 Hz whereas the jump-down freqeuncies occurred in the range of 19.3 Hz to 25.1 Hz. The jump-down frequencies shifted to the left whereas the jump-up frequencies shifted to the right for every increment of 1.0 mm gap between the magnets.

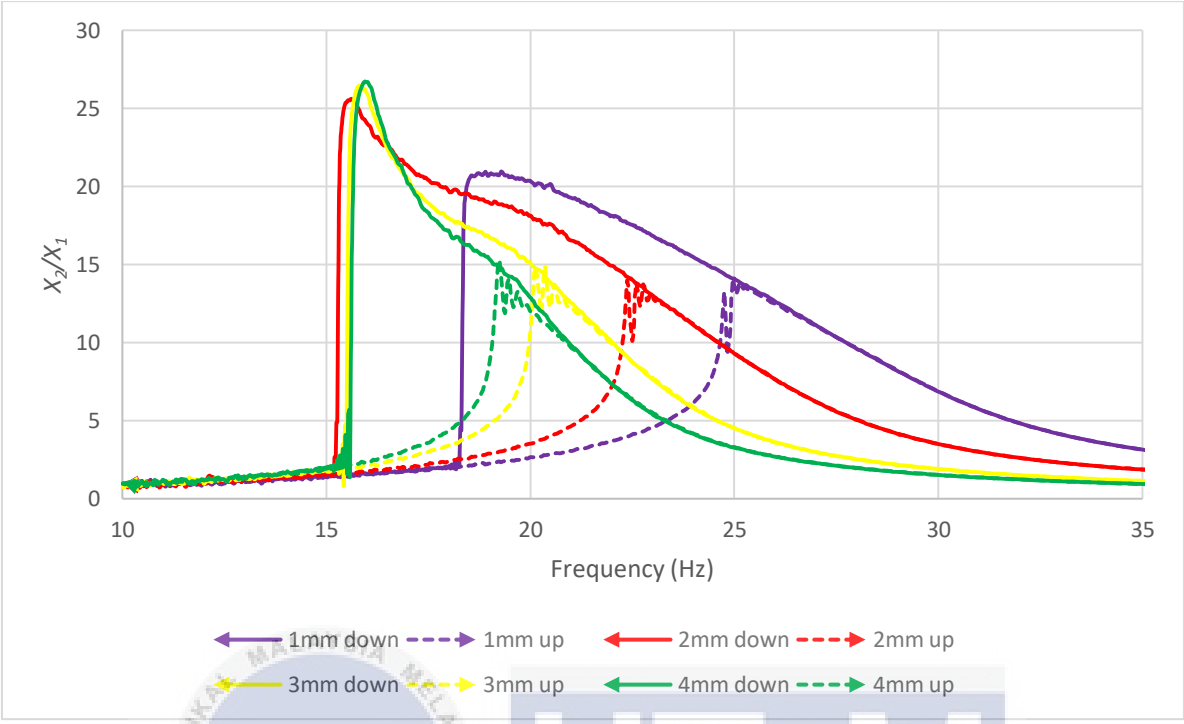

Figure 4.8: Graph of of $\frac{X_2}{X_1}$ *against* f under a constant input excitation of 1.0 mm (peak).

Figure 4.9 shows the graph of $\frac{X_2}{X_1}$ against f under a constant input excitation of 1.5 mm. The jump-up freqeuncies occurred in the range of 13.6 Hz to 14.5 Hz whereas the jump-down freqeuncies occurred in the range of 18.1 Hz to 24.5 Hz. The jump-down frequencies shifted to the left whereas the jump-up frequencies shifted to the right for every increment of 1.0 mm gap between the magnets.

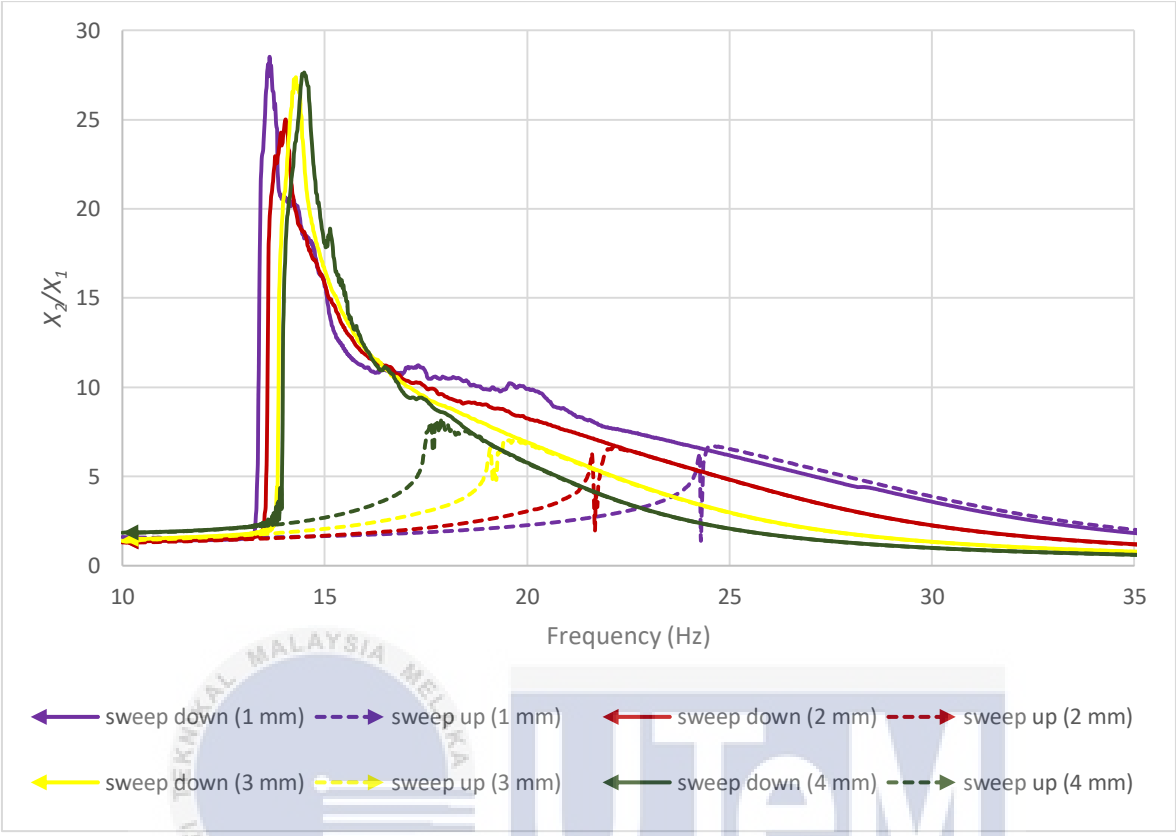

Figure 4.9: Graph of of $\frac{X_2}{X_1}$ *against* f under a constant input excitation of 1.5 mm (peak).

4.4.2.2 Effect of Different Gap for Attractive Configuration

Figure 4.10 shows the graph of of $\frac{X_2}{X_1}$ against f under a constant input excitation of 0.5 mm. The response curves bend to the right indicate that the mechanism of the device showed a hardening behaviour. The dashed lines represent a sweep up frequency from 10 Hz to 35 Hz while the solid lines represent a sweep down frequency from 35 Hz to 10 Hz. The device showed the similar behaviour for the jump-up and jump-down as the repulsive configuration. However, the gap 1.0 mm showed a softening curve for both sweep up and sweep down frequency. This is another type of nonlinear behaviour which is called the bi-stable mechanism. Ramlan et al. (2012) obtained the same behaviour for the hardening mechanism when the separation gap between two attractive magnets was small. This was due to the input level used was not high

enough to throw the mass between the two stable positions. The device showed a hardening behaviour at the gap 2.0 mm, 3.0 mm and 4.0 mm. The curves bend more to the right during a sweep up frequency compare to sweep down frequency. The jump-up freqeuncies occurred in the range of 15.8 Hz to 20.3 Hz whereas the jump-down freqeuncies occurred in the range of 16.3 Hz to 22.5 Hz. The jump-up and jump-down frequencies shifted to the right for every increment of 1.0 mm gap between the magnets.

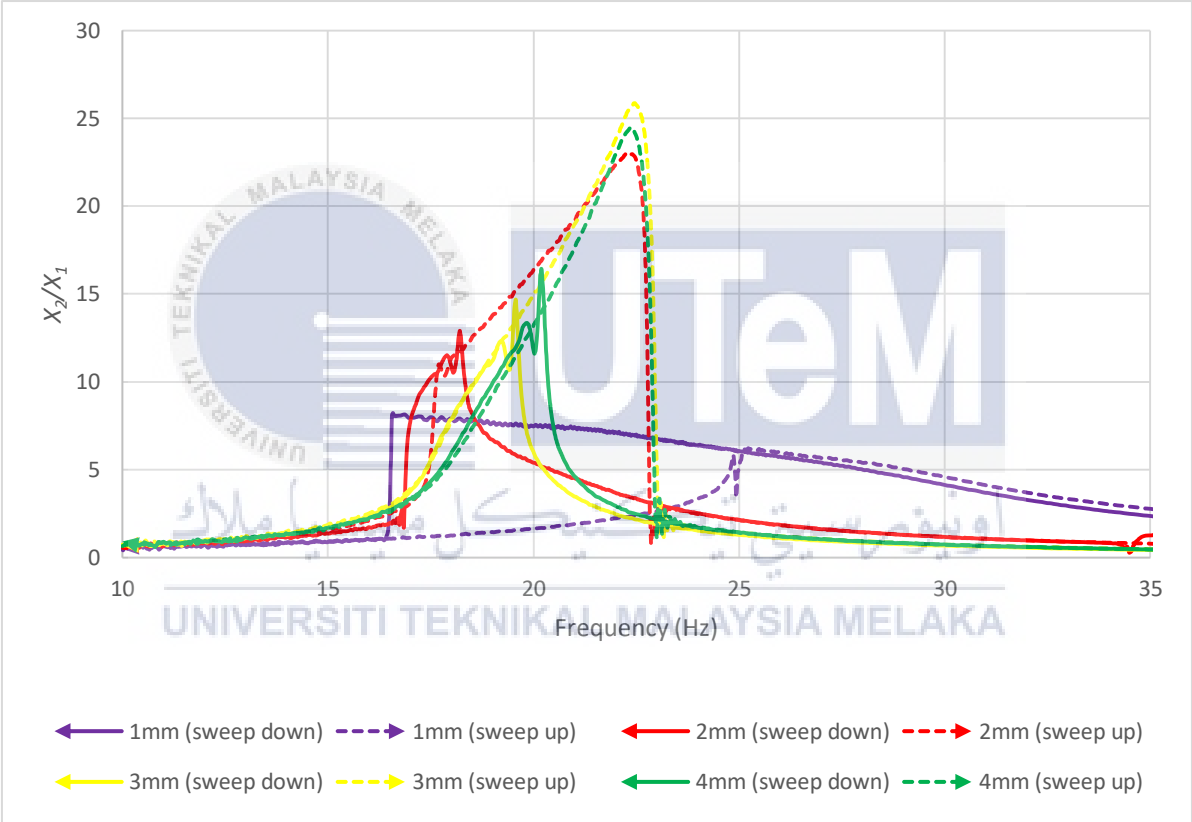

Figure 4.10: Graph of of $\frac{X_2}{X_1}$ *against* f under a constant input excitation of 0.5 mm (peak).

Figure 4.11 shows the graph of of $\frac{X_2}{X_1}$ against f under a constant input excitation of 1.0 mm. The gap 1.0 mm showed a softening curve for both sweep up and sweep down frequency. The jump-up freqeuncies occurred in the range of 15.4 Hz to 21.3 Hz whereas the

jump-down freqeuncies occurred in the range of 19.0 Hz to 24.0 Hz. The jump-up and jump-down frequencies shifted to the right for every increment of 1.0 mm gap between the magnets.

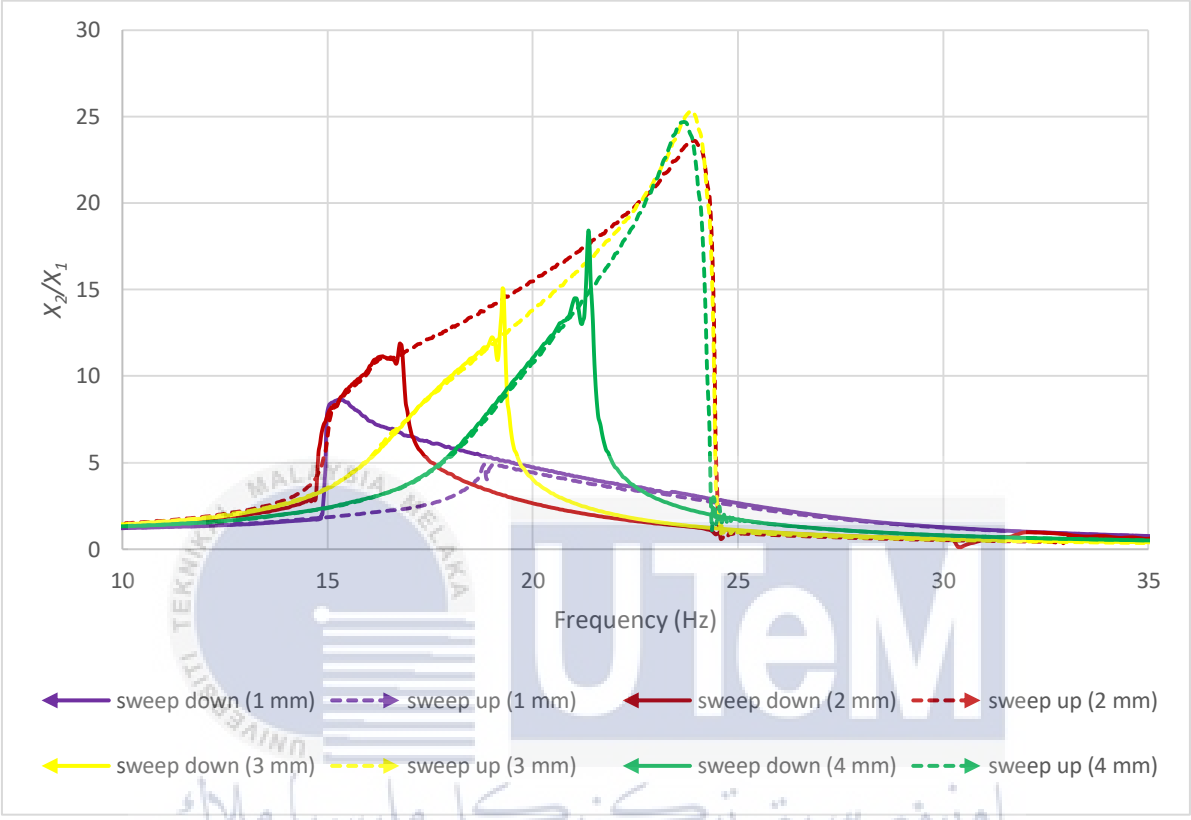

Figure 4.11: Graph of of $\frac{X_2}{X_1}$ *against* f under a constant input excitation of 1.0 mm (peak).

Figure 4.12 shows the graph of of $\frac{X_2}{X_1}$ against f under a constant input excitation of 1.5 mm. The gap 1.0 mm showed a softening curve for both sweep up and sweep down frequency. The jump-up freqeuncies occurred in the range of 16.1 Hz to 22.1 Hz whereas the jump-down freqeuncies occurred in the range of 18.1 Hz to 23.9 Hz. The jump-up and jump-down frequencies shifted to the right for every increment of 1.0 mm gap between the magnets.

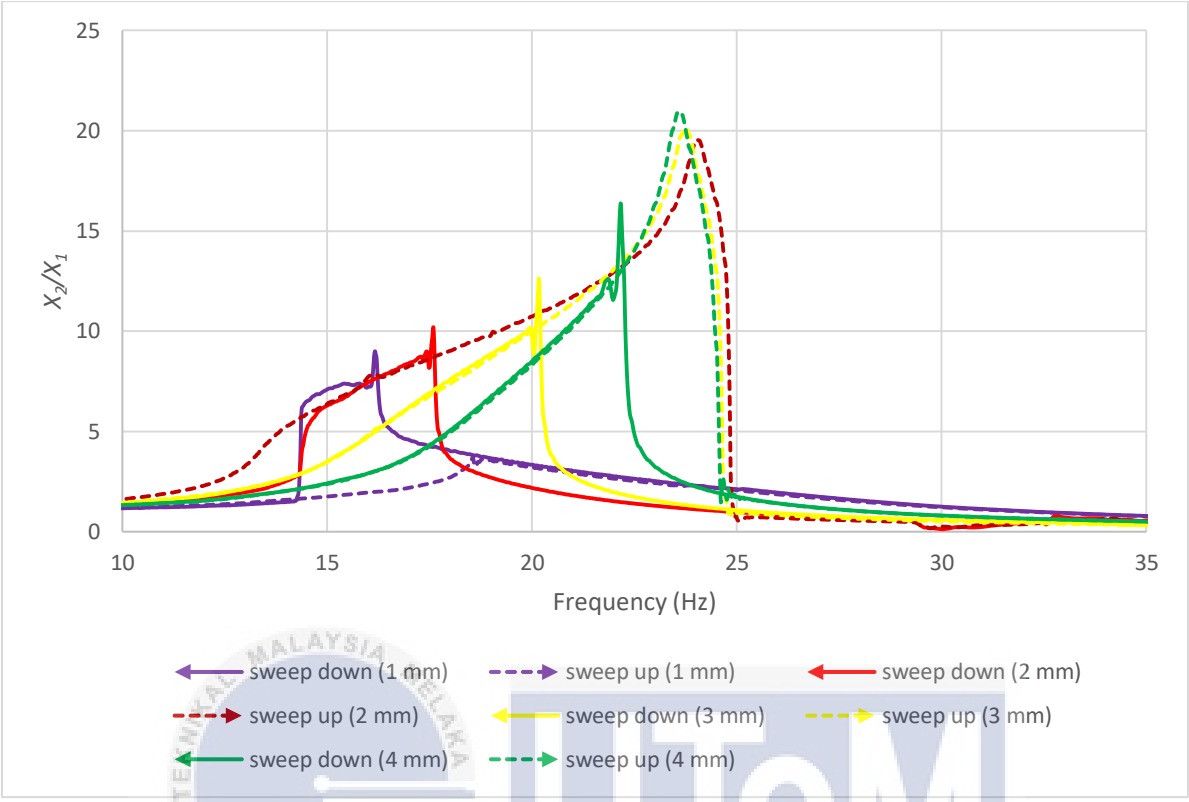

Figure 4.12: Graph of of $\frac{X_2}{X_1}$ *against* f under a constant input excitation of 1.5 mm (peak).

Table 4.3: The jump-up and jump-down frequencies for dynamic measurement.

Configuration	Input Excitation (peak), X_1 (mm)	Gap, y (mm)	Jump-Up Frequency (Hz)	Jump-Down Frequency (Hz)	Nature of NDVA
Repulsive (N-N)	0.5	1.0	17.5	27.1	Softening
		2.0	15.7	24.1	Softening
		3.0	15.3	21.3	Softening
		4.0	14.8	19.5	Softening
	1.0	1.0	18.7	25.1	Softening
		2.0	15.7	23.7	Softening

		3.0	15.8	19.7	Softening
		4.0	16.1	19.3	Softening
	1.5	1.0	13.6	24.5	Softening
		2.0	14.3	21.8	Softening
		3.0	14.4	19.8	Softening
		4.0	14.5	18.1	Softening
Attractive (N-S)	0.5	1.0	17.1	18.7	Softening
		2.0	15.8	16.3	Softening
		3.0	18.7	20.8	Hardening
		4.0	20.3	22.5	Hardening
	1.0	1.0	15.4	19.0	Softening
		2.0	17.3	23.4	Hardening
		3.0	19.4	24.0	Hardening
		4.0	21.3	23.8	Hardening
	1.5	1.0	16.1	18.1	Softening
		2.0	17.6	23.9	Hardening
		3.0	20.1	23.8	Hardening
		4.0	22.1	23.7	Hardening

4.4.2.3 Effect of Different Input Excitation for Repulsive Configuration

Figure 4.13 shows the graph of $\frac{X_2}{X_1}$ against f under a constant gap of 3.0 mm with different input excitation of 0.5 mm, 1.0 mm and 1.5 mm. The dashed lines represent a sweep up frequency from 10 Hz to 35 Hz while the solid lines represent a sweep down frequency from

35 Hz to 10 Hz. The jump-up freqeuncies occurred in the range of 14.4 Hz to 15.3 Hz whereas the jump-down freqeuncies occurred in the range of 19.8 Hz to 21.3 Hz. The jump-up and jump-down frequencies shifted to the left and the ratio of $\frac{X_2}{X_1}$ decreased for every increment of input excitation. This phenomena can be explained by the data obtained in quasi-static measurement where the degree of the nonlinearity has increased as the input excitation level has increased. Therefore, the increase in input excitation will results in increase in the jump-up and jump-down frequency which is the degree of the nonlinearity.

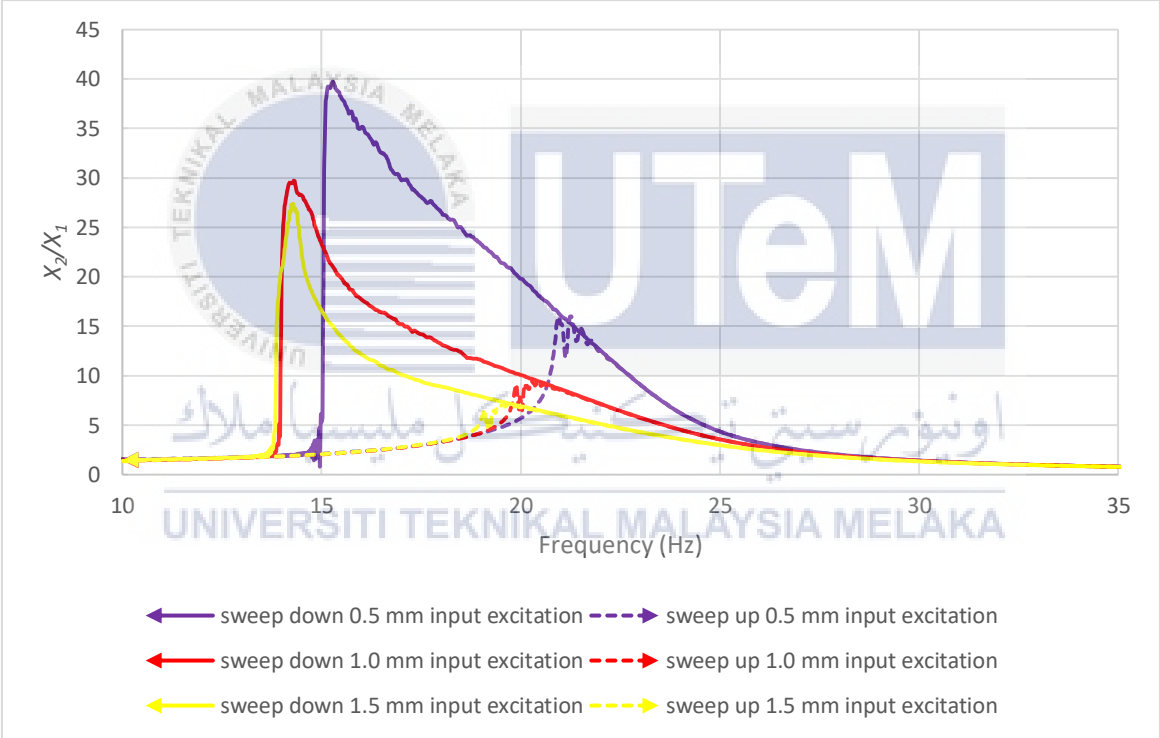

Figure 4.13: Graph of of $\frac{X_2}{X_1}$ *against* f under a constant gap of 3.0 mm with different input excitation for repulsive configuration.

4.4.2.4 Effect of Different Input Excitation for Attractive Configuration

Figure 4.14 shows the graph of of $\frac{X_2}{X_1}$ against f under a constant gap of 3.0 mm with different input excitation of 0.5 mm, 1.0 mm and 1.5 mm. The dashed line represents sweep up

frequency from 10 Hz to 35 Hz whereas the solid line represents a sweep down frequency from 35 Hz to 10 Hz. The jump-up freqeuncies occurred in the range of 18.7 Hz to 20.1 Hz whereas the jump-down freqeuncies occurred in the range of 20.8 Hz to 23.8 Hz. The jump-up and jump-down frequencies shifted to the right and the ratio of $\frac{X_2}{X_1}$ decreased for every increment of input excitation. This phenomena can be explained by the data obtained in quasi-static measurement where the degree of the nonlinearity has increased as the input excitation level has increased. Therefore, the increase in input excitation will results in increase in the jump-up and jump-down frequency which is the degree of the nonlinearity.

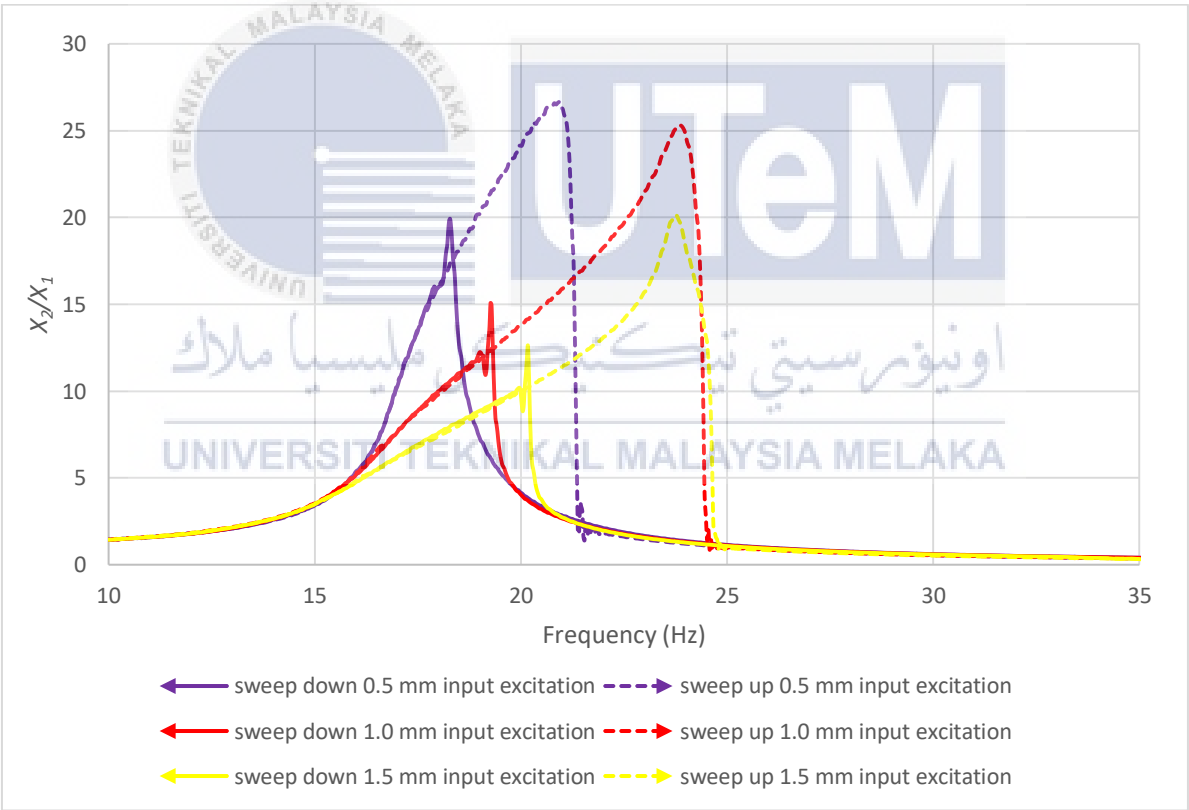

Figure 4.14: Graph of of $\frac{X_2}{X_1}$ $against$ f under a constant gap of 3.0 mm with different input excitation for repulsive configuration.

4.4.3 Performance Measurement of the LDVA and NDVA on the Beam Structure

This section discussed the performance of the LDVA and NDVA. Each device was attached on the beam structure which first natural frequency is 20 Hz as shown in Figure 4.15. The reduction bandwidth from each experiment to compare the performance between the LDVA, single NDVA and combined NDVA.

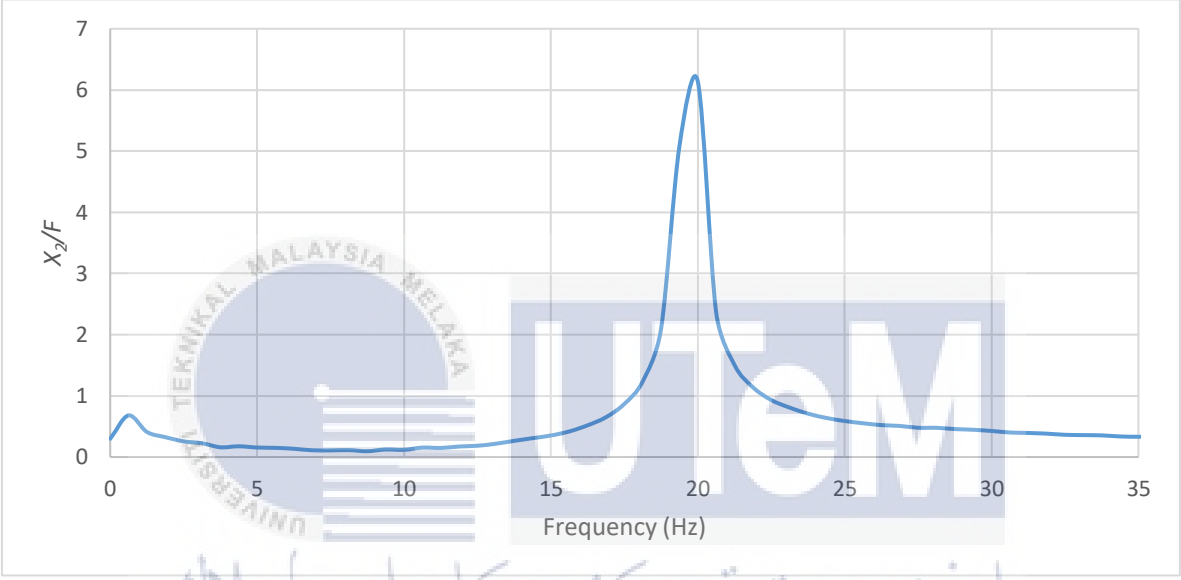

Figure 4.15: First natural frequency of the beam structure.

4.4.3.1 Performance of the LDVA on the Beam Structure

Figure 4.16 shows the FRF of the primary structure with linear vibration absorber which has been tuned to match the first natural frequency of the structure at 20 Hz. The performance of the linear absorber is evaluated at the frequency reduction bandwidth of $\frac{X}{F} < 0.1$. From the graph, the LDVA has successfully reduced the vibration at the beam resonance frequency at 20 Hz to a significant level. The reduction bandwidth of LDVA is from 18.9 Hz to 20.9 Hz which is 2 Hz.

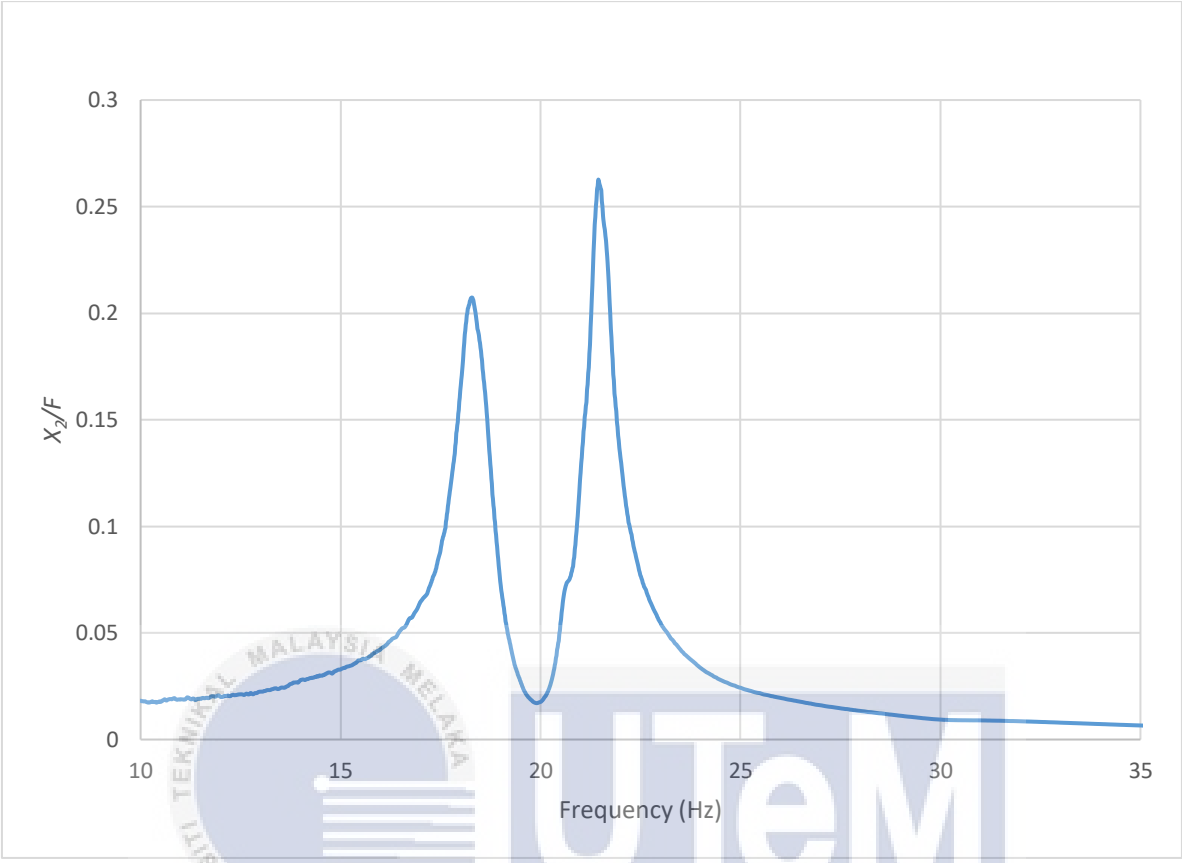

Figure 4.16: Performance of the LDVA.

4.4.3.2 Performance of the NDVA with Softening Stiffness Mechanism on the Beam Structure

Figure 4.17 and figure show the frequency response function of sweep up and sweep down profile for nonlinear vibration absorber of repulsive configuration. The frequency reduction bandwidth of $\frac{X}{F} < 0.1$ are tabulated in Table 4.4. The input excitation from the shaker is kept constant at 1 mm while changing the gap between the magnet. For sweep up test, the 1.0 mm gap failed to produce a reduction bandwidth of $\frac{X}{F} < 0.1$ at the natural frequency of the beam at 20 Hz. Therefore, the 1.0 mm gap is not effective for softening mechanism vibration absorber in reducing the structure beam at resonance during sweep up test. The 2.0 mm gap

produced the largest reduction bandwidth which is 2.8 Hz whereas the 4.0 mm gap produced the smallest reduction bandwidth which is 1.7 Hz. For sweep down test, the 2.0 mm gap produced the largest reduction bandwidth which is 6.1 Hz whereas the 4.0 mm gap produced the smallest reduction bandwidth which is 4.9 Hz. Generally, it can be seen that the nonlinear vibration absorber of softening mechanism gives a better performance during the sweep down test as they produced an overall larger bandwidth. The reason for this could be possibly due to the frequency response curves of the softening mechanism bend more to the left during sweep down frequency compare to sweep up frequency as shown in the dynamic measurement experiment. By looking at the trend, it can be concluded that the bandwidth is reduced as the gap increases. The vibration absorber is losing its softening mechanism effect and approaching a linear behavior instead as the magnets were brought farther apart.

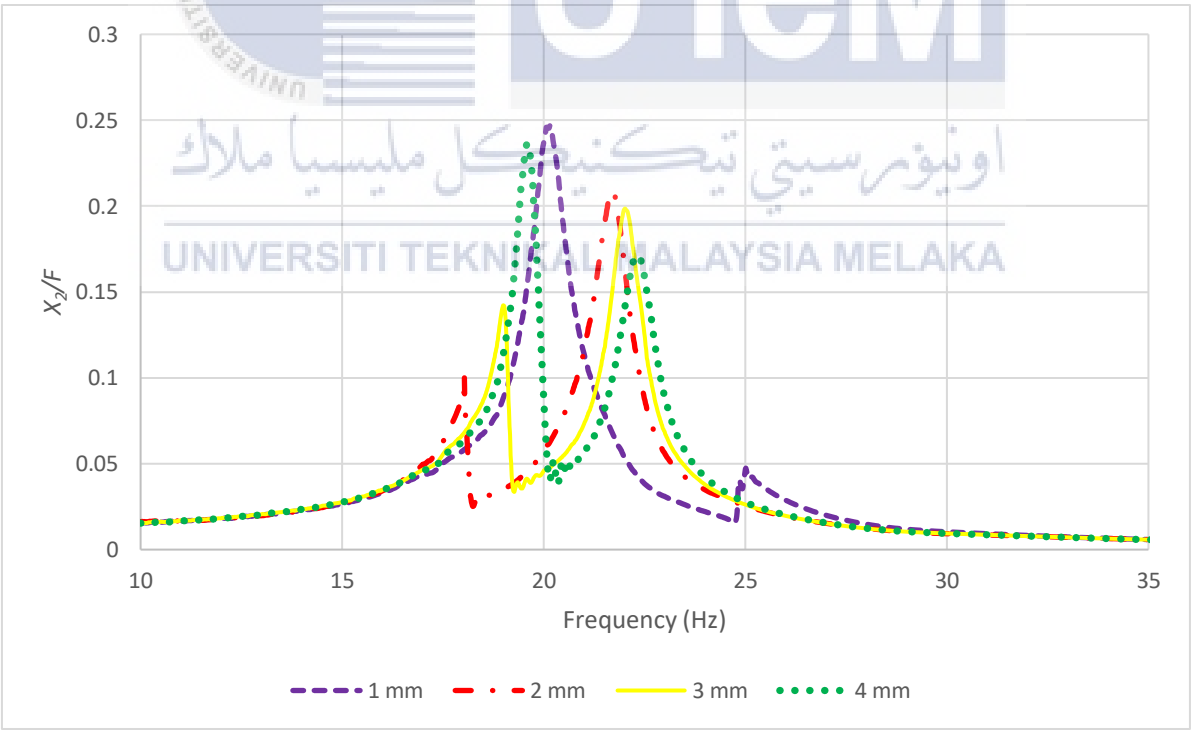

(a)

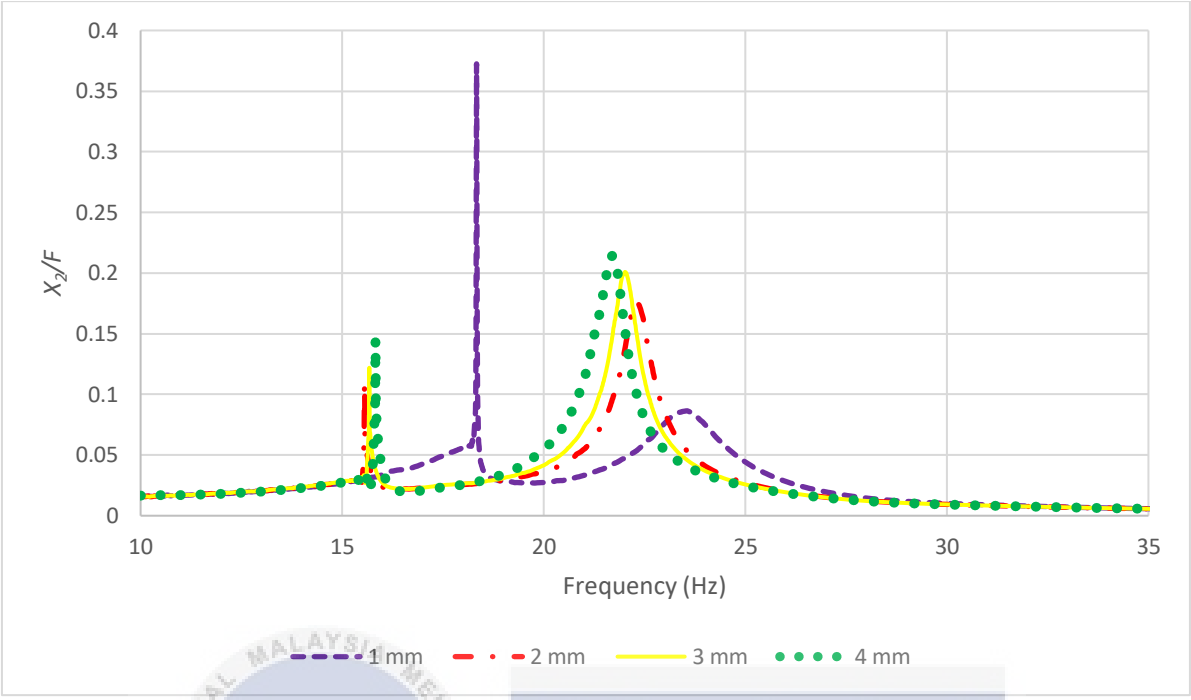

(b)

Figure 4.17: Performance for NDVA with softening stiffness mechanism (a) sweep up (b) sweep down.

Table 4.4: Vibration reduction bandwidth for NDVA with softening stiffness mechanism.

Sweep profile / Gap, y (mm)	Vibration reduction bandwidth (Hz)	
	Sweep up	Sweep down
1.0	21.4 – 25.0	18.3 – 23.6
2.0	18.0 – 20.8	15.6 – 21.7
3.0	19.1 – 21.4	15.8 – 21.4
4.0	20.0 – 21.7	15.9 – 20.8

4.4.3.3 Performance of the NDVA with Hardening Stiffness Mechanism on the Beam Structure

Figure 4.18(a) and (b) show the frequency response function of sweep up and sweep down profile for nonlinear vibration absorber of attractive configuration. The frequency reduction bandwidth of $\frac{X}{F} < 0.1$ are tabulated in Table 4.5. The input excitation from the shaker is kept constant at 1.0 mm while changing the gap between the magnet. For sweep up test, the 1.0 mm gap failed to produce a reduction bandwidth of $\frac{X}{F} < 0.1$ at the natural frequency of the beam at 20 Hz. Therefore, the 1.0 mm gap is not effective for hardening mechanism vibration absorber in reducing the structure beam at resonance during sweep up test. The 2.0 mm gap produced the largest reduction bandwidth which is 4.5 Hz whereas the 4.0 mm gap produced the smallest reduction bandwidth which is 3.2 Hz. For sweep down test, the 1.0 mm gap produced the largest reduction bandwidth which is 2.8 Hz whereas the 4.0 mm gap produced the smallest reduction bandwidth which is 2.2 Hz. Generally, it can be seen that the nonlinear vibration absorber of hardening mechanism gives a better performance during the sweep up test as they produced an overall larger bandwidth. The reason for this could be possibly due to the frequency response curves of the hardening mechanism bend more to the right during sweep up frequency compare to sweep down frequency as shown in the dynamic measurement experiment. By looking at the trend, it can be concluded that the bandwidth is reduced as the gap increases. It is thought that the effect of nonlinearity is decreasing and approaching a linear behavior instead as the magnets were brought farther apart.

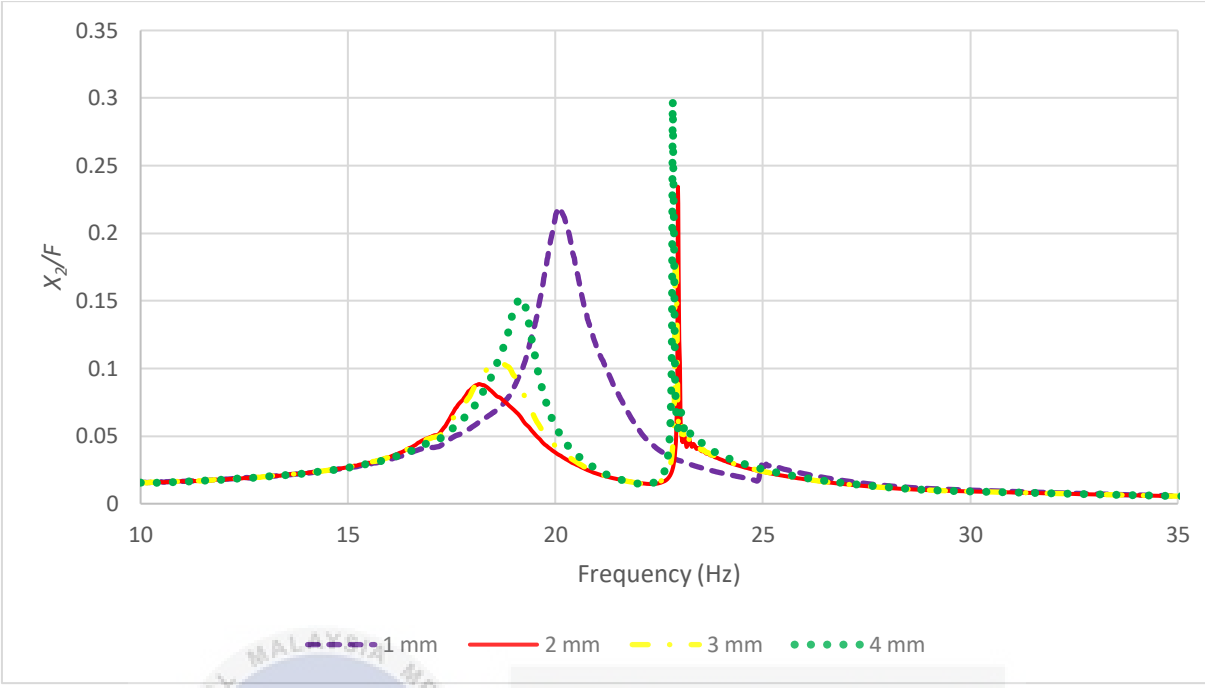

(a)

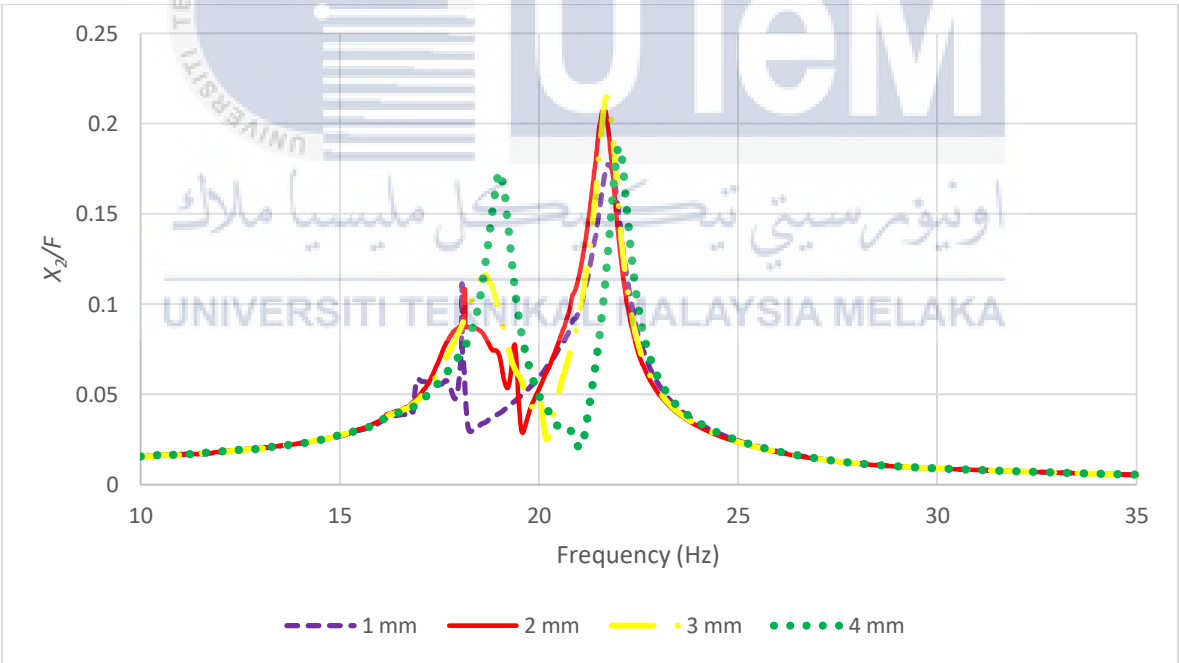

(b)

Figure 4.18: Performance for NDVA with hardening stiffness mechanism (a) sweep up (b) sweep down.

Table 4.5: Vibration reduction bandwidth for NDVA with hardening stiffness mechanism.

Sweep Profile / Gap, y (mm)	Vibration reduction bandwidth (Hz)	
	Sweep up	Sweep down
1.0	21.3 – 25	18.2 – 21.0
2.0	18.3 – 23.0	18.2 – 20.8
3.0	18.3 – 22.8	19.0 – 21.1
4.0	19.6 – 22.8	19.5 – 21.6

4.4.3.4 Performance of the NDVA with Combined Softening and Hardening Stiffness Mechanism on the Beam Structure

Two nonlinear vibration absorbers of hardening and softening mechanism are attached on the beam to test the performance of the combined system. Only 2.0 mm gap is set for test since it is the only configuration that able to reduce the resonance of the beam at 20 Hz compare to other gaps. The same test for sweep up and sweep down are ran at the same input excitation of 1.0 mm. The results are shown in Figure 4.19.

Figure 4.19 (a) and (b) show the frequency response function of sweep up and sweep down profile for both combined nonlinear vibration absorber. The frequency reduction bandwidth of $\frac{X}{F} < 0.1$ are tabulated in Table 4.6. The reduction bandwidth of the combined of both mechanisms produced a reduction bandwidth of 4.6 Hz for the sweep up test and 6.3 Hz for the sweep down test. The performance test shows that the combined of both nonlinear vibration absorbers have performed well in reducing the natural frequency of the beam during both sweep up and sweep down frequencies. This is because the combined system has both of

the benefits from the hardening mechanism during the sweep up frequencies and softening mechanism during the sweep down frequencies.

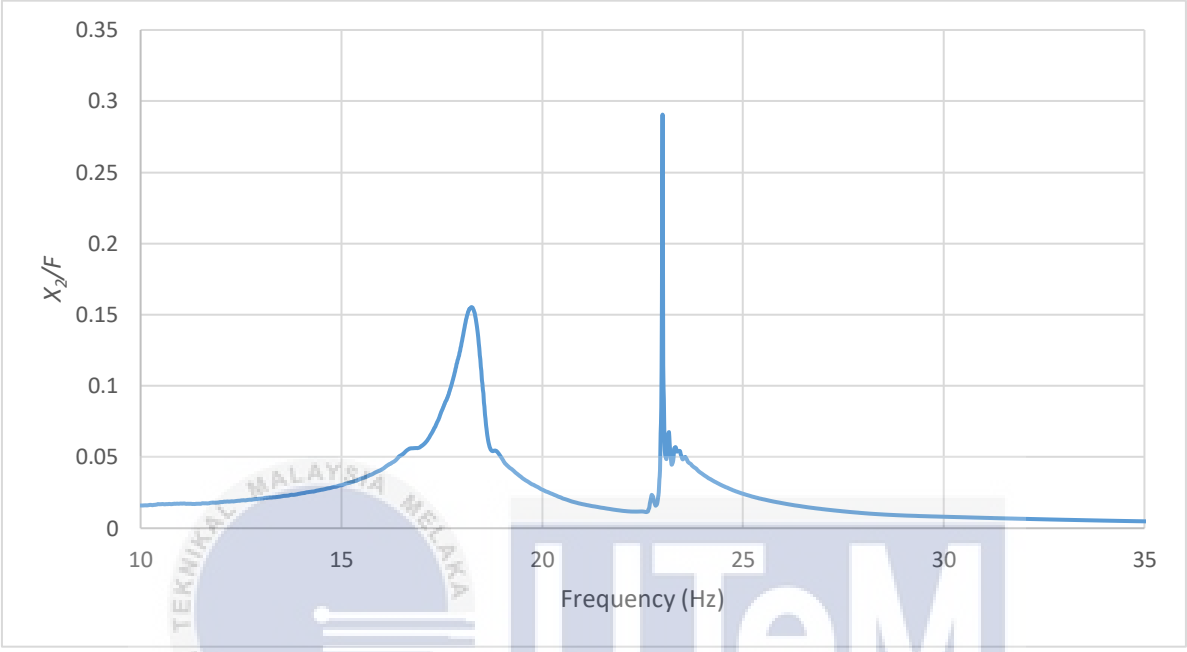

(a)

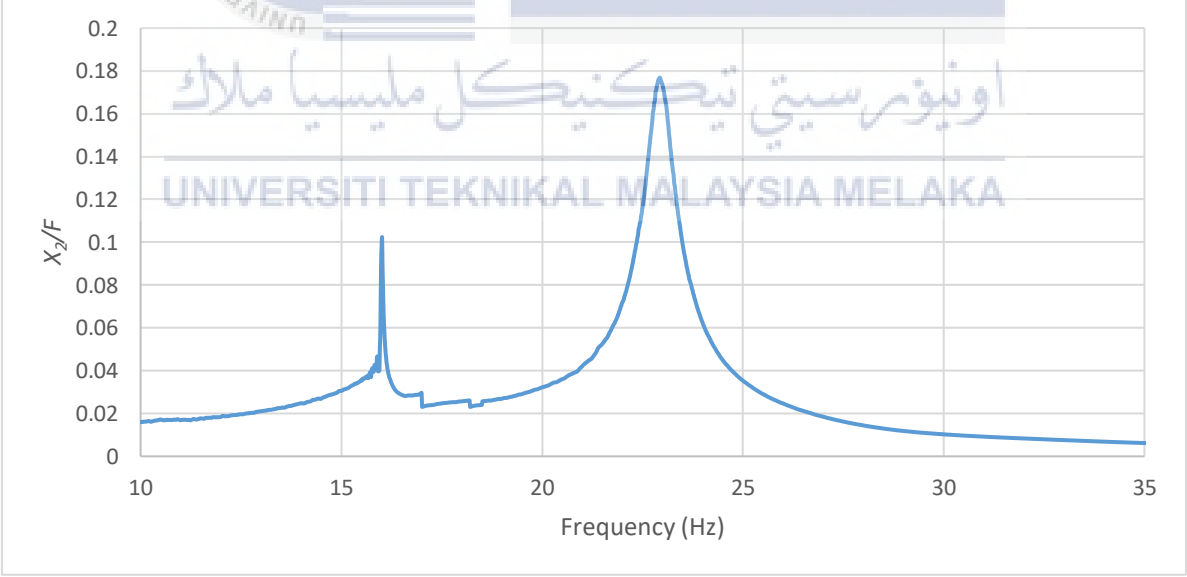

(b)

Figure 4.19: Performance for NDVA with combined softening and hardening stiffness mechanism (a) sweep up (b) sweep down.

Table 4.6: Vibration reduction bandwidth for NDVA with combined softening and hardening stiffness mechanism.

Sweep Profile / Gap, *y* (mm)	Vibration reduction bandwidth (Hz)	
	Sweep Up	Sweep Down
2.0	18.5 – 23.1	16.0 – 22.3

4.4.3.5 Comparison of the Performance between LDVA, Individual NDVA and Combined NDVA

Table 4.7 shows the summary of the best performance result from each test. Figure 4.20 shows the summary chart of the best performance result from each test. The performance of linear vibration absorber is the lowest compare to the nonlinear vibration absorber as its bandwidth is only 2.0 Hz. The nonlinear vibration absorber of hardening mechanism and the combined of both mechanisms produced the largest bandwidth during sweep up test which is 4.5 Hz. However, the vibration absorber with only hardening mechanism produced a low bandwidth during a sweep down test which is 2.8 Hz. The nonlinear vibration absorber of softening mechanism produced a larger bandwidth during sweep down test which is 6.1 Hz. However, it produced a low bandwidth during a sweep up test which is only 2.8 Hz. For combined of both nonlinear mechanisms vibration absorbers, they produced the largest bandwidth for sweep down test which is 6.3 Hz. It can be concluded that the combined of both nonlinear vibration absorber has a better performance compare to hardening or softening vibration absorber in both sweep up and sweep down test with a large reduction bandwidth.

Table 4.7: Comparison of the performance between LDVA, individual NDVA and combined NDVA.

Vibration absorber	Vibration reduction bandwidth at level below 0.1 (Hz)	
	Sweep up (bandwidth)	Sweep down (bandwidth)
Linear	2.0	2.0
Hardening	4.5	2.8
Softening	2.8	6.1
Hardening + Softening	4.5	6.3

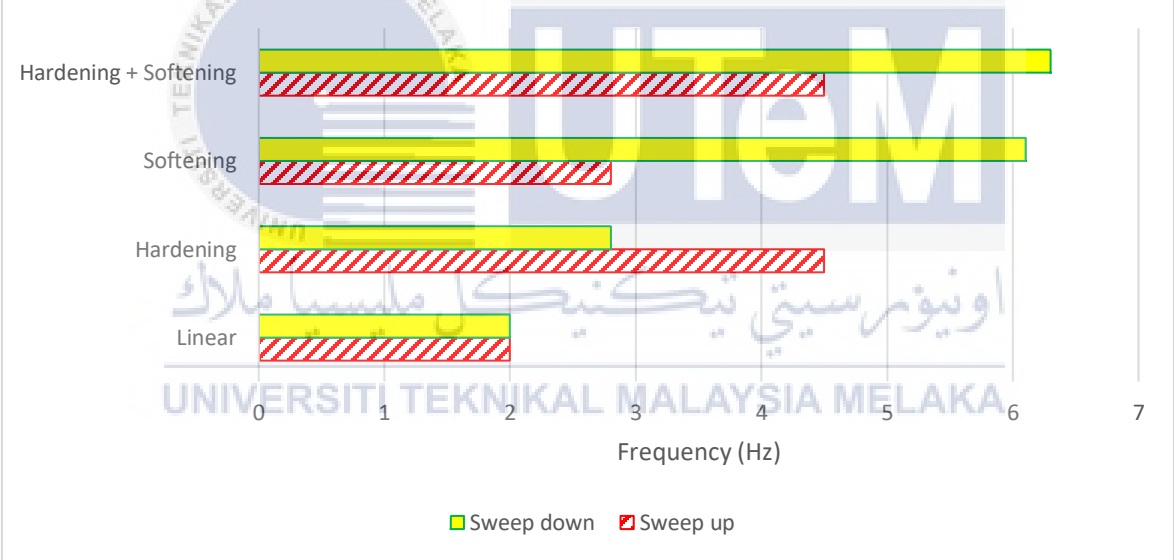

Figure 4.20: Performance chart of LDVA, individual NDVA and combined NDVA.

4.5 Conclusions

Throughout this chapter, a results on the experimental study of a passive linear and nonlinear vibration absorber has been presented. The nonlinearity of the absorber was due to the interaction force between the magnets where repulsive configuration will induce softening

mechanism and attractive configuration will induce hardening mechanism. The quasi-static measurement shows that the nonlinearity of the absorber can be altered by adjusting the separation gap between the magnets. The closer the magnets the higher the nonlinearity of the absorber. In the dynamic measurement, the NDVA showed a jump-down phenomena during sweep up frequency and a jump-up phenomena during sweep down frequency. It was found that the jump-up and jump-down frequencies were altered as the gap was adjusted. The bandwidth for the shorter gap was larger compare to the larger gap. The input excitation level also affected the nonlinear behavior of the device. The nonlinearity was found to be higher when the input excitation was increased as shown by the response curve which shifted to form larger bandwidth area. For comparison, there was a good agreement between quasi-static and dynamic measurement. From the force-deflection graph, it can be seen that the region with a lower amplitude excitation was linear. As the excitation increases, the curves look more obvious for both softening and hardening. The measured performance for the NDVA produced a wider vibration reduction bandwidth compare to the LDVA. The softening mechanism produced a larger reduction bandwidth during the sweep down frequency whereas the hardening mechanism produced a larger reduction bandwidth during sweep up frequency. One reason found is the behavior observed during the dynamic test where the softening mechanism produced a larger bandwidth was larger during sweep down frequency whereas the hardening mechanism produced a larger bandwidth during sweep up frequency. The combined NDVA with both softening and hardening mechanism did not produce a much wider vibration bandwidth as those with the single NDVA. However, the benefit of the combined NDVA is the larger reduction bandwidth during sweep up and sweep down frequency.

CHAPTER 5

CONCLUSION & RECOMMENDATION

5.1 Conclusion

Many researches were carried out to study the nonlinear vibration absorber. This thesis has been taken an interest in which the nonlinearity produced by the nonlinear absorber stiffness will benefits in a vibration absorber. Passive vibration absorber is found to have a greater preferences compare to the other approach due to its low cost, simplicity and reliability. The experimental results for a LDVA and NDVA of softening and hardening stiffness mechanism were presented and discussed. The finding of this research are summarized in the following.

. The nonlinear stiffness was produced by the magnets. The NDVA operates in softening system when the magnets are arranged in a repulsive configuration and operates in hardening system when the magnets are arranged in an attractive configuration. The nonlinear stiffness can be altered by adjusting the separating gap between the magnets at the tip mass and at the slider block. The device was tuned to the first natural frequency of the beam structure which was obtained through theoretical prediction and impact test.

Quasi-static measurement was conducted to study the relationship between restoring force against tip deflection for softening and hardening stiffness. For softening, the restoring force decreases as the tip deflection increases whereas for hardening the restoring force increases as the tip deflection increases. It was found that both of the nonlinear stiffness decreases as the

separation gap increases. In other word, the nonlinear device is approaching a linear behavior as the separation gap increases.

The effect of the nonlinearity (i.e. separation gap) and the input excitation on the dynamics of the system was investigated for the NDVA. The NDVA exhibits jump-down phenomena during sweep up frequency and jump-up phenomena during sweep down frequency. It was found that the device for both softening and hardening system has a higher bandwidth when the nonlinearity and input excitation was increased. For a hardening system, the device behaves as a softening system at 1.0 mm gap for every input excitation. This nonlinear behavior is called bi-stable mechanism and it is not covered in this research scope.

The NDVA has a wider effective reduction bandwidth compared to a LDVA. Compared to the LDVA, the NDVA has the effect of shifting the second resonance peak to a higher frequency away from the tuned frequency, which improves the robustness of the device to mistune. However, the NDVA with softening system only has a wider reduction bandwidth during sweep down test whereas for the NDVA with hardening system only has a wider reduction bandwidth during the sweep up test. By combining both of the softening and hardening system, the reduction bandwidth was slightly wider for both sweep up and sweep down test.

The research presented in this thesis has improved the understanding of the characteristics and effects of the NDVA and its capability on the vibration reduction. The NDVA was designed to tune the nonlinear stiffness by adjusting the separation gap between the magnets.

5.2 Recommendations for Future Works

For future research, it will be interesting to make the tuning of the damping is possible so that the effect of damping could be investigated. Further research could be carried out to investigate the benefits of the bi-stable mechanism. Another recommendation is to determine the effect of NDVA parameters on the vibration reduction bandwidth and effective tuned frequency with analytical expressions since they have not been investigated in this thesis. Last but not least, conduct an investigation using combined softening and hardening stiffness mechanism using different method to induce the nonlinearity.

REFERENCES

Aida, Y., Niewa, H., Maeda, Y., 1994. Dynamics Vibration Absorber. US. Pat. 5896961.

Al-Shideifat, M.A., 2014. Asymmetric Magnet-Based Nonlinear Energy Sink. Journal of Computational Nonlinear Dynamic. 10, 014502.

Alsuwaiyan, S.A., 2015. Design and Analysis of a Simple Nonlinear Vibration Absorber 11, pp. 84–90.

Brewer, G.A., Marion, Mass, 1975. Dynamics Vibration Absorber. US Pat 4,150,588.

Carter, W.J., Liu, F.C., 1961. Steady-State Behavior of Nonlinear Dynamic Vibration Absorber. Journal of Applied Mechanic. 28, pp. 67–70.

Choy, P.K., Huang, J., Xing, X., Yung, H.Y., 2017. Active Vibration Absorber. US. Pat. 9,689.453.

Den Hartog, J.P., 1956. Mechanical Vibrations, 3rd ed. NewYork. McGraw-Hill Book Company, INC.

Fischer, O., 2007. Wind-Excited Vibrations-Solution by Passive Dynamic Vibration Absorbers of Different Types. Journal of Wind Engineering and Industrial Aerodynnamics. 95,pp. 1028–1039.

Frahm, H., 1911. Device for Damping Vibration Bodies. U.S Patent No. 989958.

Gafsi, W., Chaari, R., Masmoudi, N., Khabou, M.T., Chaari, F., Haddar, M., 2017. Modeling of a Passive Absorber in Milling Tool Machine. Applied Acoustic. 128, pp. 94–110.

Gao, X., Chen, Q., 2013. Active Vibration Control for A Bilinear System with Nonlinear Velocity Time-delayed Feedback, The World Congress on Engineering.

Gatti, G., Brennan, M.J., Kovacic, I., 2010. On the Interaction of the Responses at the Resonance Frequencies of a Nonlinear Two Degrees-of-Freedom System. Physica. D Nonlinear Phenomena. 239, pp. 591–599.

Gourc, E., Michon, G., Seguy, S., Berlioz, A., 2015. Targeted Energy Transfer Under Harmonic Forcing With a Vibro-Impact Nonlinear Energy Sink: Analytical and Experimental Developments. Journal of Vibration Acoustic. 137, 031008, pp. 9-25.

Habib, G., Kerschen, G., 2016. A principle of similarity for nonlinear vibration absorbers 332, pp. 1–8.

Habib, G., Kerschen, G., Stepan, G., 2017. Chatter Mitigation Using the Nonlinear Tuned Vibration Absorber. International Journal of Nonlinear Mechanics. 91, pp. 103–112.

Hsu, Y., 2003. The performance of a nonlinear dynamic vibration absorber. University of Southampton, UK.

Huang, X., Su, Z., Hua, H., 2018. Application of a Dynamic Vibration Absorber with Negative Stiffness for Control of a Marine Shafting System. Ocean Engineering. 155, pp. 131–143

Hunt, J.B., Nissen, J.C., 1982. The Broadband Dynamic Vibration Absorber. Journal of Sound and Vibration. 83, pp. 573–578.

Inman, D.J., 2011. Engineering Vibrations, 4th ed, Pearson. New Jersey: Pearson Education, INC. Upper Saddle River.

Jiang, X., Michael Mcfarland, D., Bergman, L.A., Vakakis, A.F., 2003. Steady State Passive

Nonlinear Energy Pumping in Coupled Oscillators: Theoretical and Experimental Results. Nonlinear Dynamic. 33, pp. 87–102.

Jo, H., Yabuno, H., 2009. Amplitude Reduction of Primary Resonance of Nonlinear Oscillator by a Dynamic Vibration Absorber Using Nonlinear Coupling. Nonlinear Dynamics. 55, pp. 67–78.

Kojima, H., Saito, H., 1983. Forced Vibrations Dynamic of a Beam Vibration With a Non Linear. Journal of Sound Vibration. 88, pp. 559–568.

Lee, Y.S., Nucera, F., Vakakis, A.F., McFarland, D.M., Bergman, L.A., 2009. Periodic Orbits, Damped Transitions and Targeted Energy Transfers in Oscillators With Vibro-Impact Attachments. Physica D Nonlinear Phenomena. 238, pp. 1868–1896.

Mohanty, S., Dwivedy, S.K., 2016. Linear and Nonlinear Analysis of Piezoelectric Based Vibration Absorber with Acceleration Feedback. Procedia Engineering. 144, pp. 584–591.

Nissen, J.C., Popp, K., Schmalhorst, B., 1985. Optimization of a Non-Linear Dynamic Vibration Absorber Sound Vibration 99, pp. 149–154.

Pennisi, G., Mann, B.P., Naclerio, N., Stephan, C., Michon, G., 2018. Design and experimental study of a Nonlinear Energy Sink coupled to an Electromagnetic Energy Harvester. Journal of Sound Vibration 437, pp. 340–357.

Pirner, M., 2002. Actual Behaviour of a ball Vibration Absorber. Journal of Wind Engineering and Industrial Aerodynamics. 90, pp. 987–1005.

Poon, D.C.K., Shieh, S., Joseph, L.M., Chang, C., 2004. Structural Design of Taipei 101, The World's Tallest Building. Proc. CTBUH 2004 Seoul Conf. Seoul, Korea 271–278.

Ramlan, R., Brennan, M.J., Kovacic, I., Mace, B.R., Burrow, S.G., 2016. Exploiting Knowledge of Jump-Up and Jump-Down Frequencies to Determine the parameters of a Duffing Oscillator. Communications in Nonlinear Science and Numerical Simulatoin. 37, pp. 282–291.

Ramlan, R., Brennan, M.J., MacE, B.R., Burrow, S.G., 2012. On the Performance of a Dual-Mode Non-Linear Vibration Energy Harvesting Device. Journal of Intelligent Material System and Structures. 23, pp. 1423–1432.

Rice, H.J., McCraith, J.R., 1987. Practical Non-Linear Vibration Absorber Design. Topics in Catalysis. 116, pp. 545–559.

Roberson, R.E., 1952. Synthesis of a Nonlinear Dynamic Vibration Absorber. Journal of the Franklin Institute. 254, pp. 205–220.

Roberto, W., Godoy, A. De, Trindade, M.A., 2015. Parametric Analysis of a Nonlinear Dynamic Vibration Absorber Based on Snap-Through Geometry. Carlos School of Engineering.

Schilling, D.R., 2013. What Caused The Bangladesh Building To Collapse Killing Over 800? Industrial Tap.

Silva, T.M.P., Clementino, M.A., Erturk, A., De Marqui Junior, C., 2018. An Experimentally Validated Piezoelectric Nonlinear Energy Sink for Wideband Vibration Attenuation. Journal of Sound Vibration. 437, pp. 68–78.

Soltani, P.S., Kerschen, G., 2015. The Nonlinear Piezoelectric Tuned Vibration Absorber. Smart Materials and Structures. 24, 75015.

Sun, C., Eason, R.P., Nagarajaiah, S., Dick, A.J., 2013. Hardening Düffing Oscillator Attenuation Using a Nonlinear TMD, a Semi-Active TMD and Multiple TMD. Journal of Sound

Vibration. 332, pp. 674–686.

Sun, J.Q., Jolly, M.R., Norris, M.A., 1995. Passive, Adaptive and Active Tuned Vibration Absorbers. A Survey Journal of Vibration Acoustic. 117, pp. 234.

Tang, B., Brennan, M.J., Gatti, G., Ferguson, N.S., 2016. Experimental Characterization of a Nonlinear Vibration Absorber Using Free Vibration. Journal of Sound Vibration. 367, pp. 159–169.

Vlab.amrita.edu, 2011. Free Vibration of a Cantilever Beam (Continuous System) [online]. Availabe at: http://vlab.amrita.edu/?sub=3&brch=175&sim=1080&cnt=1 [Accessed on 11 October 2018).

Yamakawa, I., Takeda, S., Kojima, H., 1977. Behavior of a New Type Dynamic Vibration Absorber Consisting of Three Permanent Magnets. Bulletin of the JSME 20, pp. 947–954.